
Director's Discretionary Fund Report for Fiscal Year 1995

Ames Research Center

March 1996



National Aeronautics and
Space Administration

Director's Discretionary Fund Report for Fiscal Year 1995

Ames Research Center, Moffett Field, California

March 1996



National Aeronautics and
Space Administration

Ames Research Center
Moffett Field, CA 94035-1000

Contents

	Page
Introduction	vii
Section 1: Final Reports	
Robust Nonlinear Control and Guidance System Design Methods	1
<i>Victor H. L. Cheng, Chima E. Njaka, and P. K. Menon</i>	
Intervertebral Disc and Back Pain Studies Using Spinal Traction and Compression during Magnetic Resonance Imaging	3
<i>Alan R. Hargens, Richard E. Ballard, Klaus P. Fechner, Karen J. Hutchinson, Gita Murthy, Douglas F. Schwandt, Donald E. Watenpaugh, and Jacqueline M. William</i>	
Computational Fluid Dynamics Simulation of Left Ventricular Assist Device	7
<i>Dochan Kwak and Cetin Kiris</i>	
A Study of Atmospheric Sampling by Supersonic Aircraft	9
<i>Stephen R. Langhoff and Henry G. Adelman</i>	
Organic Matter from H ₂ O and CO ₂ Dissolved in Minerals	10
<i>Narcinda R. Lerner, Friedemann Freund, Alka Gupta, Devendra Kumar, Scott A. Sandford, and Max P. Bernstein</i>	
The Opacity of Water Vapor	13
<i>Harry Partridge and David Schwenke</i>	
Deep Near-Infrared Cosmological Surveys	15
<i>Thomas L. Roellig, Edwin F. Erickson, Jacqueline A. Davidson, and Arati Chokshi</i>	
Does the Collapse of Diatom Blooms Trigger Coccolithophore Blooms?	17
<i>Lynn Rothschild</i>	
Improving Future Space Missions by Capitalizing on Aeropass Maneuvers of the Magellan Spacecraft	20
<i>Paul Wercinski, Brian Haas, and Robert Tolson</i>	
Orbiting Infrared Spectral Flux Calibrators	22
<i>Eliot Young and Fred Witteborn</i>	
Section 2: Ongoing Reports	
Waterproofing the Space Shuttle Tiles	25
<i>Charles W. Bauschlicher, Jr.</i>	
Thermal Protection Systems for Reusable Vehicles	26
<i>Jeffrey V. Bowles, Henry Adelman, and Mark Loomis</i>	
Planar Interferometric Measurement of Skin Friction	27
<i>James L. Brown and Jonathan Naughton</i>	

Computer Modeling of the Thermal Conductivity of Cometary Ice	28
<i>Theodore E. Bunch, Michael A. Wilson, and Andrew Pohorille</i>	
The Use of Nitrous Oxide to Increase Test Times in High-Enthalpy Reflected Shock Tunnels	29
<i>John Cavolowsky, Mark Newfield, David W. Bogdanoff, Gregory J. Wilson, Myles A. Sussman, Richard J. Exberger, and William E. Warren</i>	
Ultrasensitive Detection of Atmospheric Free Radical Molecules: A Full-Sensitivity Demonstration Prototype	31
<i>Charles Chackerian, Christopher R. Mahon, James R. Podolske, and Thomas Blake</i>	
Isotopic Analysis of Meteoritic Organosulfur and Organophosphorous Compounds	32
<i>Sherwood Chang and George Cooper</i>	
Development of Fiber-Optic Sensors for Studies of Transition from Laminar to Turbulent Flow	34
<i>Y. C. Cho, N. N. Mansour, and R. D. Mehta</i>	
Size-Density Studies of Chondrules, and Aerodynamic Sorting in the Solar Nebula	35
<i>Jeff Cuzzi, Julie Paque, and Monica Rivera</i>	
Effects of Stratospheric Ozone Depletion and Increased Levels of Ultraviolet Radiation on Plants of Arizona	36
<i>Hector L. D'Antoni, Joseph W. Skiles, Jeraldine Mazzurco, Dan Levy, and Heather Brady</i>	
Return to the Red Planet: Remote Sensing Analog Studies as Preparation for Mars Exploration Exobiology	37
<i>Jack D. Farmer and James Brass</i>	
Laser-Spectroscopic Instrument for Turbulence Measurements	39
<i>Douglas G. Fletcher</i>	
Biotechnical Applications of Reusable Surface Insulation	40
<i>Howard E. Goldstein and Daniel B. Leiser</i>	
Computational Modeling of Ultrafast Optical Pulse Propagation in Semiconductor Lasers and Amplifiers	41
<i>Peter M. Goorjian, Govind P. Agrawal, Andrew Hulse, Andre Knoesen, and John Heritage</i>	
A Long-Duration Test Flight of a Superpressure Balloon as a Platform for Mars Exploration	43
<i>Robert M. Haberle, G. Scott Hubbard, Lawrence G. Lemke, Geoffrey A. Briggs, and James Cantrell</i>	
Remote Sensing of Aircraft Contrails Using a Field Portable Imaging Interferometer	44
<i>Philip D. Hammer, William H. Smith, Stephen Dunagan, and Anthony Strawa</i>	
Development of Noninvasive, Tissue-Oxygen Sensor for Optimizing Ergonomic Design of Workstations in Space and on Earth	45
<i>Alan R. Hargens, Gita Murthy, Norman J. Kahan, David M. Rempel, Yvonne A. Clearwater, and Bruce W. Webbon</i>	
A Novel Telemetric Biosensor to Monitor Blood pH Online	48
<i>John W. Hines, Sara B. Arnaud, Chris Soms, Marc Madou, Lynn Kim, Jennifer Garrison, and Michael Harrison</i>	

Global Climate Change: The Role of Electron-CO ₂ Collisions in the Cooling of the Thermosphere	50
<i>Winifred M. Huo</i>	
Understanding Ion Mobility in Polymer Electrolytes for Lithium-Polymer Batteries.....	51
<i>Richard L. Jaffe, Grant D. Smith, and Harry Partridge</i>	
Residential Fireplace Density Measurement Using Airborne Multispectral Scanners	52
<i>Jeff Jenner</i>	
Turbulent Boundary Layer Measurements on Transport Wing Wind-Tunnel Models	53
<i>Dennis A. Johnson and Jeffrey D. Brown</i>	
Validation of Engine-change Procedures through Team Task Analysis	54
<i>Barbara G. Kanki and Diane Walter</i>	
Nonlinear Interactions between Background Disturbances and Disturbances Generated by Laminar Flow Control Devices	55
<i>Lyndell S. King and Jonathan H. Watmuff</i>	
Ground-based Photometric Detection of Terrestrial-sized Extrasolar Planets	56
<i>David Koch and Laurance Doyle</i>	
Practical Evaluation of a New Method to Reduce Helicopter Rotor Hub Loads	58
<i>Sesi Kottapalli, Inderjit Chopra, and Judah Milgram</i>	
Development of an Automated Telescope Balancing System for the Kuiper Airborne Observatory/Stratospheric Observatory for Infrared Astronomy	59
<i>Robert W. Mah, Alex Galvagni, Ramin Eshaghi, Robert Curlee, and Barry Fujii</i>	
Planar Doppler Velocimetry	60
<i>Robert L. McKenzie</i>	
A Microwave-Pumped GaAs Far Infrared Photoconductor	62
<i>Robert E. McMurray, Jr., Jam Farhoomand, and Nick Scott</i>	
Design Optimization Using Automated Differentiation and Parallel Decomposition	63
<i>Hirokazu Miura, Ilan Kroo, and Steve Altus</i>	
A Search Technique for Discovering Earth-crossing Comets from Meteor Stream Outbursts and Determining Their Orbits in Space	65
<i>David Morrison, Peter Jenniskens, H. Betlem, H. Mostert, M. C. de Lignie, K. Jobse, and I. Yrjola</i>	
Ultra-light Entry Vehicle Development	67
<i>Marcus S. Murbach and Demetrius Kourtides</i>	
Using Ecosystem Science and Technology to Balance the Conservation of Water Supply and Native Hawaiian Rainforests	68
<i>Robyn Lee Myers</i>	
A New Method for Measuring Cloud Liquid Water Using Near Infrared Remote Sensing	70
<i>Peter Pilewski</i>	

Computation of the Low-temperature Rate Constants for the Reaction $\text{HO}_2 + \text{O}_3 \rightarrow \text{OH} + \text{O}_2 + \text{O}_2$	71
<i>David W. Schwenke and Stephen P. Walch</i>	
A New Method to Test Rotor Hover Performance	72
<i>Mark Silva and Frank Caradonna</i>	

Introduction

The Director's Discretionary Fund (DDF) at Ames Research Center was established to fund innovative, high-risk projects in basic research that are essential to our future programs but otherwise would be difficult to initiate. Summaries of individual projects within this program are compiled and issued by Ames each year as a NASA Technical Memorandum.

These summaries cover 10 final and 36 ongoing projects in Fiscal Year 1995.

The contents are listed alphabetically according to the last name of the primary investigator in two sections (final and ongoing reports). Following the narrative reports, two appendixes (for final and ongoing reports) contain brief descriptions with the financial distribution and status of each of the projects.

Any questions can be addressed to an investigator directly.

SECTION 1

FINAL REPORTS

Robust Nonlinear Control and Guidance System Design Methods

Investigator(s)

Victor H. L. Cheng,
Ames Research Center,
Moffett Field, CA 94035-1000

Other personnel involved

Chima E. Njaka, Ames Research Center
P. K. Menon, Santa Clara University,
Santa Clara, CA 95053

Objectives of the study

To investigate methods for designing nonlinear control systems that can tolerate substantial variations in the plant parameters without becoming unstable or suffering significant degradation in performance, for the automation of aircraft guidance and control. In particular,

- to understand the source of performance degradation due to uncertainties in a realistic aircraft model;
- to develop design methods for controllers that can provide robust performance under some bounded nonlinear system uncertainties; and
- to evaluate the design techniques to verify the improvement in robustness over existing controller designs.

Progress and results

The overall approach makes use of theories in singular perturbation, state-dependent nonlinear inverse, and robust control design, as well as the use of a high-fidelity simulation system for the aircraft as a valuable resource for analysis and synthesis. Within this general framework, two specific approaches were studied for designing the state-dependent nonlinear inverse, and two approaches were considered for the robust control design. A helicopter control problem was selected as the application to evaluate these approaches because of the criticality of robust performance and stability of helicopters in ground-hugging nap-of-the-Earth (NOE) flight: the attitude control of the UH-60A Black Hawk helicopter. The GenHel simulation model serves as the high-fidelity simulation system for the UH-60A.

The first approach for designing the state-dependent nonlinear inverse involved the extraction of a pseudolinear aerodynamic model from the high-fidelity simulation based on off-line computation. The pseudolinear aerodynamic model was then used as the

basis for designing the resulting nonlinear inverse. Figure 1 illustrates the control feedback structure involving the nonlinear inverse of the first approach. The second approach made use of the high-fidelity simulation as an embedded system to obtain an affine model of the aircraft dynamics online in real time, and then the affine model was used as the basis for designing the resulting nonlinear inverse. Figure 2 illustrates the control feedback structure involving the nonlinear inverse of the second approach.

Preliminary analysis of these two approaches revealed that both are successful in linearizing the system, and both exhibit a small degree of mismodeling of the nonlinear inverse to completely linearize the high-fidelity simulation model. Figure 3 contains a sample response of the roll-angle feedback loop based on a nonlinear inverse with a simple proportional-plus-derivative linear controller. The nonlinear inverse from the first approach was chosen to carry on the robust control design study.

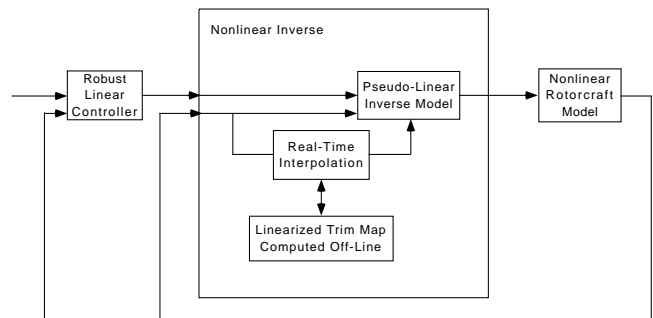


Figure 1. Control feedback structure with pseudolinear nonlinear inverse.

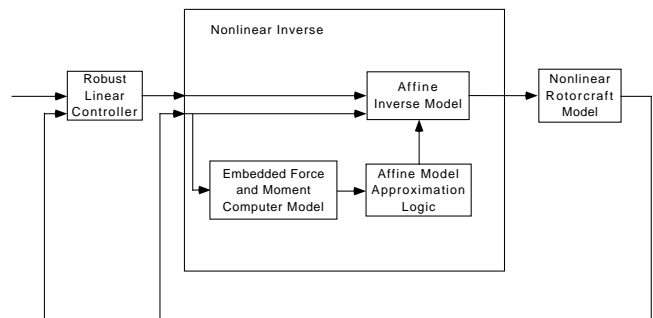


Figure 2. Control feedback structure with real-time affine model nonlinear inverse.

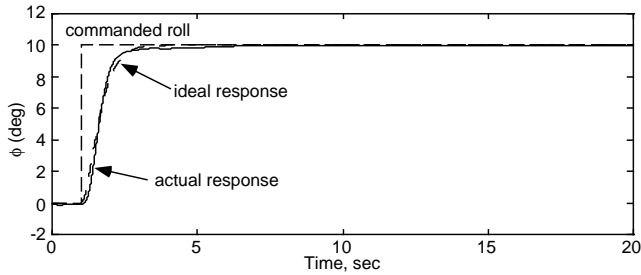


Figure 3. Sample response of roll angle to roll command.

Two techniques were considered for the robust control design, and both used high-fidelity simulation to characterize the effect of the modeling error on the nonlinear-inverse controller towards the synthesis of the robust controller. The first approach was based on a frequency-domain formulation, and it used H_∞ and μ -synthesis tools for the design, while the second approach was based on a time-domain formulation, and the design was based on a differential-game framework. Figure 4 illustrates the frequency response of the inner-loop feedback system based on the nonlinear inverse and that of a perfectly linearized system. The synthesis of these robust controllers continues, and the results will be documented in a future paper.

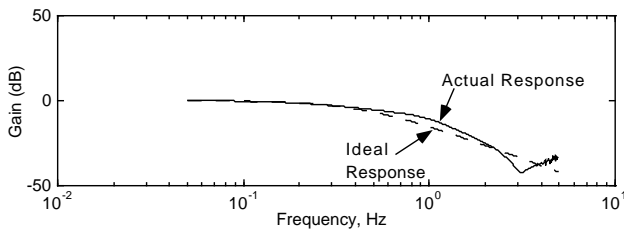


Figure 4. Frequency response of roll angle to roll command.

Significance of the results

During the process of studying the integration of nonlinear inverse design and robust controller design to obtain nonlinear robust controllers for full-envelope operation, it has become evident that a high-fidelity

simulation system for the aircraft is an invaluable asset for the analysis and synthesis of the system. First, both approaches for synthesizing the nonlinear inverse controller are based on the high-fidelity simulation model: the first approach uses it to generate the pseudolinear aerodynamic model, whereas the second approach actually includes the high-fidelity simulation as an embedded system.

Furthermore, the high-fidelity simulation is used to analyze the resulting inner-loop system to characterize the effectiveness of the nonlinear inverse and the resulting mismatch with an ideal linear system. Analysis of the nonlinear-inverse controller suggests that, because of the approximation introduced by linearization of the force and moment aerodynamics, the overall closed-loop system does not behave entirely like a linear time-variant system. Hence model uncertainty is inherent in this closed-loop system. This system serves as a good starting point to evaluate the full robust controller, which should provide improved performance under such model uncertainty.

Publications resulting from study

1. Njaka, C. E.; Menon, P. K.; and Cheng, V. H. L.: Towards an Advanced Nonlinear Rotorcraft Flight Control System Design. Paper presented at the 13th IEEE/AIAA Digital Avionics Systems Conference, Phoenix, Ariz., Oct. 30–Nov. 3, 1994, pp. 190–197.
2. Menon, P. K.; Njaka, C. E.; and Cheng, V. H. L.: Nonlinear Flight Control Using Embedded Vehicle Computer Model. Paper presented at the AIAA Guidance, Navigation, and Control Conference, Baltimore, Md., Aug. 7–9, 1995.
3. Cheng, V. H. L.; Njaka, C. E.; and Menon, P. K.: Practical Design Methodologies for Robust Nonlinear Flight Control. Submitted to the 13th World Congress of the International Federation of Automatic Control, San Francisco, Calif., July 1–5, 1996.

Keywords

Guidance and control, Nonlinear controller, Robust controller

Intervertebral Disc and Back Pain Studies Using Spinal Traction and Compression during Magnetic Resonance Imaging

Investigator(s)

Alan R. Hargens, Ames Research Center,
Moffett Field, CA 94035-1000
Richard E. Ballard, University of California,
San Diego, Ames Research Center
Klaus P. Fechner, Stanford University,
Palo Alto, CA 94305-4035
Karen J. Hutchinson, University of California,
San Diego, Ames Research Center
Gita Murthy, University of California, San Diego,
Ames Research Center
Douglas F. Schwandt, V. A. Medical Center,
Palo Alto, CA 94304-1200
Donald E. Watenpaugh, University of California,
San Diego, Ames Research Center
Jacqueline M. William, Ames Research Center/
Lockheed Martin Missiles & Space

Objectives of the study

The objectives of this research are twofold: 1) to design and construct a spinal compression and traction device; and 2) to use this device during magnetic resonance imaging (MRI) to study height, cross-sectional area, volume, and water content of intervertebral discs along the length of the entire spine during spinal traction and spinal compression. Traction during recumbency enables lengthening the spine by an amount (4–7 cm) similar to that documented during spaceflight (refs. 1 and 2). The compression harness during recumbency allows quantification of relationships between spinal loading and disc physiology and morphology.

Using MRI, we hypothesize that: 1) disc height, volume, and water content increases the most during recumbency with traction; and 2) stepwise increases in spinal loading with the compression harness produces decrements of spinal disc height, volume, and water content. Furthermore, spinal compression enables quantification for the first time in vivo of the basic relationship between changes in spinal loading and disc volume. These experimental results will yield a noninvasive estimate of disc compliance, where disc compliance = $\Delta\text{volume}/\Delta\text{load}$.

Progress and results

A prototype of the spinal compression/traction system was designed and built. The spinal compression component of the system consists of a wood footplate connected to shoulder pads with nylon webbing and elastic rubber bungee cords (see fig. 1). Plastic buckles in the webbing permit disconnection of the footplate and bungee cords from the upper body harness. Pulling the webbing through the buckles allows adjustment of bungee cord tension, and thus spinal compression. A transparent, graduated plastic cylinder housing the bungee cords allows calibrated stretching of the cords through adjustment of the webbing in the buckles. Harness straps balance forces at the shoulder to minimize neck constriction while reducing any tendency for the strap to slip off the shoulders. Shoulder pads also help distribute surface pressure on the shoulders and pectoral surfaces. The bungee cords function as long springs, reducing tension and providing more accurate loading over time. The compression harness can be adjusted to load the spine at specific percentages of body weight (e.g., 1/2 body weight, which is the normal load experienced by the lumbar spine while standing).

Likewise, the spinal traction component of the system was designed to apply traction load *between* the hips/legs and pectoral girdle/neck in a manner similar but opposite in direction to the spinal compression harness. Stiff members (similar to crutches) interposed between the hip/leg and underarm/neck end of the system, on either side of the subject/patient, attach to the padded hip/leg and underarm/neck assemblies via bungee cords, such that increasing the length of the members increases tension on the spine. A transparent, graduated plastic cylinder housing the bungee cords and attached to the hip belt allows calibrated stretching of the cords through adjustment of stiff-member length. A patent disclosure of the spinal traction and compression systems was recently submitted to the Ames Research Center (ARC) Office of Commercial Technology.

Six healthy male subjects underwent 3 days each of 6 deg head-down tilt (HDT) with balanced traction and horizontal bed rest (HBR), with a 2-week recovery

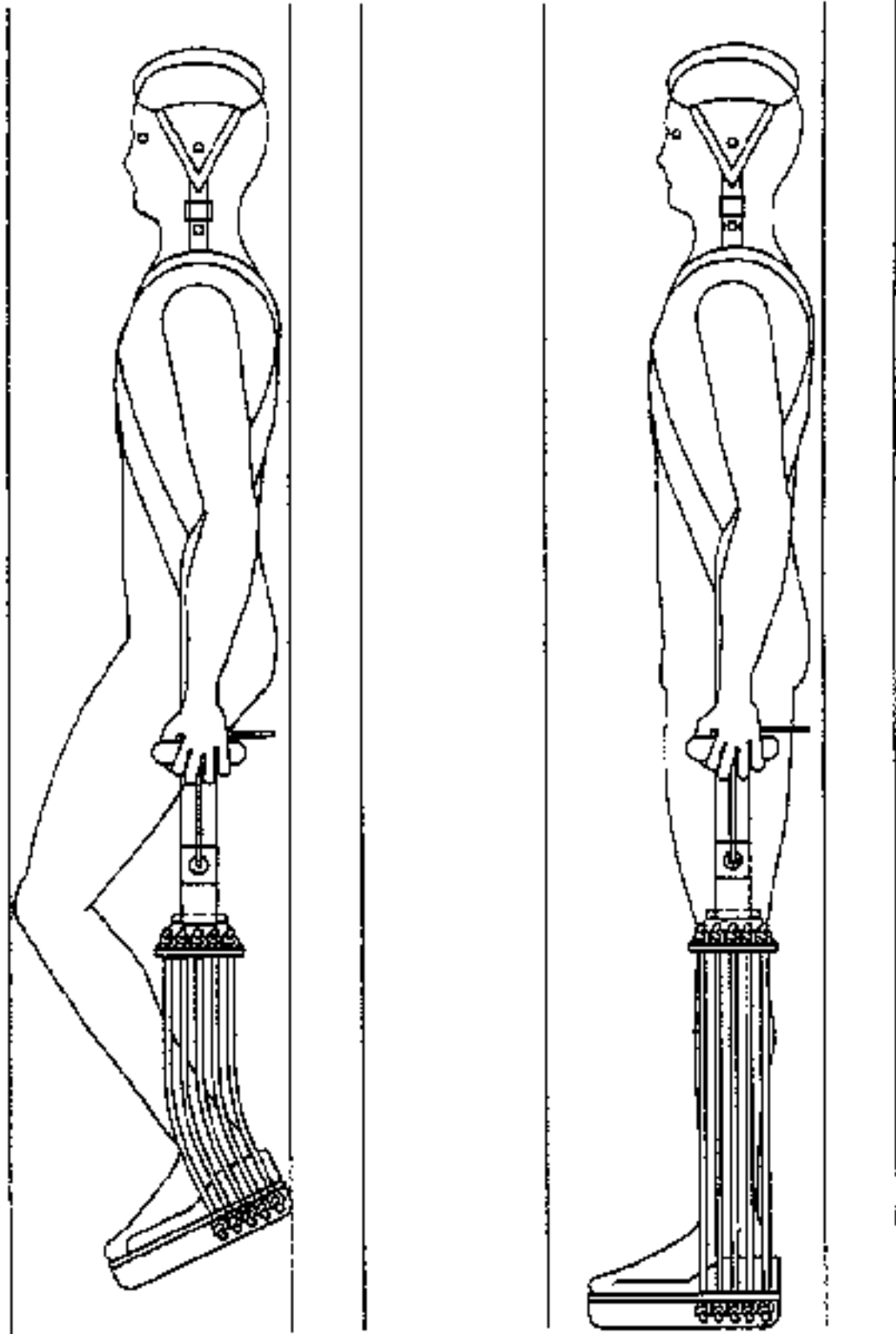


Figure 1. Spinal compression device on supine subject in MRI unit.

period between treatments. Total body and spine length, lumbar disc height, back pain, erector spinae intramuscular pressure, and ankle joint torque were measured before, during, and after each treatment. Total body and spine (processes of L5–C7) lengths increased significantly more during HDT with balanced traction (22 ± 8 mm and 25 ± 8 mm, respectively) than during HBR (16 ± 4 mm and 14 ± 9 mm, respectively). Back and leg pain were significantly greater during HDT with balanced traction than during HBR. The distance between the lower endplate of L4 and the upper endplate of S1, as measured by sonography, increased significantly in both treatments to the same degree (2.9 ± 1.9 mm, HDT with balanced traction; 3.3 ± 1.5 mm, HBR).

The spinal compression device was tested on two subjects during MRI. The subject donned the compression device in horizontal supine position and after obtaining baseline measurements with no spinal compression, the harness was tightened to compress the spine at 25-, 50-, and 75-percent body weight. Each level of compression was held for 18 to 25 minutes, with 5-minute breaks between compressions. MRIs were obtained during the last half of each spinal compression period. Preliminary results indicate that spinal shortening occurred during compression, and that a combination of intervertebral disc compression and increased spinal curvature explains this shortening.

Significance of the results

The compression and traction device will provide valuable information about the physiology of the intervertebral discs and pathophysiology of back pain in astronauts and Earthbound patients. Although there is abundant literature on intervertebral disc structure and biomechanics during spinal compression, there is no information presently available on disc morphology and physiology during spinal compression, in recumbent posture, within an MR imager. Furthermore, there is no literature available on disc morphology and physiology during spinal elongation (using traction). Disc compliance has never been quantified in vivo, yet this parameter is an important determinant of disc function because low compliance allows the disc to support weight without a large decrease in volume.

Back pain is an important clinical and economic problem in the general population, as well as a significant problem for astronauts. Back pain associated with recumbent posture on Earth may be related to back pain experienced by astronauts during spaceflight (ref. 3). Similarly, back pain reported by patients in the upright posture may be mechanistically related to the

back pain reported by some astronauts upon return to Earth. Although back pain can be attributed to some form of mechanical or pathological factor, most back pain is idiopathic (ref. 4). Therefore, research directed towards identifying causative mechanisms and aiding the treatment of back pain in patients as well as maintaining the well-being and safety of spaceflight crew members is crucial.

Publications

- Ballard, R. E.; Styf, J. R.; Watenpaugh, D. E.; Fechner, K.; Haruna, Y.; Kahan, N. J.; and Hargens, A. R.: Head-down Tilt with Balanced Traction as a Model for Simulating Spinal Acclimation to Microgravity. *American Society for Gravitational and Space Biology Bulletin*, vol. 8, no. 1, 1994, p. 19, Abstract 38.
- Haruna, Y.; Kahan, N.; Styf, J. R.; and Hargens, A. R.: Hoffman-reflex Is Delayed during 6° Head-down Tilt with Balanced Traction. Submitted to *Aviation, Space, and Environmental Medicine*, 1996.
- Styf, J. R.; Ballard, R. E.; Fechner, K.; Watenpaugh, D. E.; Kahan, N. J.; and Hargens, A. R.: Height Increase, Neuromuscular Function and Back Pain during 6° Head-down Tilt with Traction. *Aviation, Space, and Environmental Medicine*, in press, 1996.
- Styf, J. R.; Kålebo, P.; and Hargens, A. R.: Lumbar Intervertebral Disc Heights as Measured by Sonography. *Aviation, Space, and Environmental Medicine*, vol. 65, no. 5, 1994, p. 450(67).

References

1. Thornton, W. E.; Hoffler, G. W.; and Rummel, J. A.: Anthropometric Changes and Fluid Shifts. In *Biomedical Results from Skylab*, Washington, D. C., NASA SP-377, 1977, pp. 330–338.
2. Thornton, W. E.; and Moore, T. R.: Height Changes in Microgravity. In *Results of the Life Sciences DSOs Conducted Aboard the Space Shuttle 1981–1986*, M. W. Bungo, T. M. Bagian, M. A. Bowman, and B. M. Levitan, eds., NASA Johnson Space Center, Houston, Tex., 1987, pp. 55–57.
3. Hutchinson, K. J.; Watenpaugh, D. E.; Murthy, G.; Convertino, V. A.; and Hargens, A. R.: Back Pain during 6° Head-down Tilt Approximates that During Actual Microgravity. *Aviation, Space, and Environmental Medicine*, vol. 66, no. 3, 1995, pp. 256–259.

4. Ashton-Miller, J. A.; and Schultz, A. B.: Biomechanics of the Human Spine and Trunk. Exercise and Sports Science Reviews, vol. 16, 1988, pp. 169–204.

Keywords

Spinal compression, Spinal traction, Back pain, Intervertebral disc, Ultrasonography, Magnetic resonance imaging

Computational Fluid Dynamics Simulation of Left Ventricular Assist Device

Investigator(s)

Dochan Kwak, Ames Research Center,
Moffett Field, CA 94035-1000
Cetin Kiris, MCAT Institute,
Ames Research Center

Objectives of the study

To develop and apply computational fluid dynamics (CFD) tools to simulate steady and unsteady flows within artificial heart assist devices. This research is designed to provide a tool that can be used to investigate the flow of blood through a ventricular assist device (VAD). This unique insight into the internal fluid structures will lead to improved artificial devices capable of sustaining human life.

Progress and results

The design goal for an implantable left VAD (LVAD) is a small and efficient device that generates 5 liters of blood flow per minute against a 100-mm Hg pressure. Because blood is the operating fluid, the design of an LVAD requires that it propel the blood very gently; in other words, it must not damage red blood cells. In order to reduce red-blood-cell damage, the pump must be designed to prevent high-shear-stress regions and separated flow regions in the pump. In addition, the formation of blood clots may appear within stagnation regions as a result of previously damaged blood cells. The detailed computational look at the fluid flow now affords VAD designers with a view of the complicated fluid dynamic processes inside their devices.

In 1989, NASA Johnson Space Center (JSC) began a joint project with the DeBakey Heart Center of the Baylor College of Medicine (BCOM) in Houston, Texas, to develop a new, implantable LVAD prototype system. This LVAD is based on a fast rotating axial pump requiring a minimum number of moving parts. To make it implantable, the device has been made as small as possible, requiring a very high rotational speed. The flow through the baseline design of the LVAD impeller was numerically simulated by solving the incompressible Navier–Stokes equations in a steadily rotating frame of reference. The pseudocompressibility approach and zonal multiblock grids were used in these component analyses. Several design iterations were performed in order to increase hydrodynamic performances of this axial pump. First, parametric studies were performed for the optimal

impeller blade shapes and for the optimal tip clearance. Then a three-blade inducer geometry was included upstream of the impeller main blades by adopting the ideas from rocket propulsion. With the inducer addition, the efficiency of the new design was increased from 25 to 33 percent. Clinical results of the BCOM showed that the hemolysis index, which indicates the amount of blood damage, dropped from 0.02 to 0.002. The rotational speed was decreased from 12,800 to 10,800 rpm in order to generate the required blood mass flow rate.

The ideas from rocket propulsion and medical science were combined to help develop a new, implantable LVAD. Using the new computational technology, the researchers in collaboration with the JSC engineering team are investigating new design possibilities by combining a rocket engine inducer with an axial blood pump impeller. Clinical hemolysis testing and animal implantation at the BCOM have shown a remarkable improvement in performance over earlier blood pump designs.

One of the critical regions for potential blood clotting is near the bearing area between rotating and non-rotating components. Clotting can be caused in the hub area by either high shear or stagnation, depending on the gap and configuration of the area. Flows through four different bearing cavities were analyzed, and an optimum cavity geometry was suggested, which is currently in clinical testing at the BCOM.

Significance of the results

The goal of this research was to develop computational tools that could be used by the designers of mechanical heart assist devices. This computational tool now affords designers with a view of the complicated fluid dynamic processes inside their devices. Because of the nature of the devices, this detailed information cannot be obtained experimentally. The detailed computational look at the fluid flow is very important to the designers; high levels of turbulence can damage the red blood cells; and regions of recirculating flow can lead to blood clots. Thus the ability to predict these phenomena have greatly helped the designers.

In July 1991, the Institute of Medicine estimated that approximately 25,000 to 60,000 patients per year in North America could benefit from an efficient LVAD. Thus improved designs made possible because

of the current work could have a far reaching impact on human health.

Publications resulting from study

Kiris, C.; Kwak, D.; and Benkowski, B.: Computational Flow Analysis of A Left Ventricular Assist Device. Presented at 3rd Congress of The International Society for Rotary Blood Pumps, Houston, Tex., Aug. 24-27, 1995 and 6th International Symposium on CFD, Lake Tahoe, Nev., Sept. 4-8, 1995.

Keywords

Computational fluid dynamics, Incompressible flow, Left ventricular assist device (LVAD)

A Study of Atmospheric Sampling by Supersonic Aircraft

Investigators

Stephen R. Langhoff, Ames Research Center,
Moffett Field, CA 94035-1000
Henry G. Adelman, Thermosciences Institute,
Ames Research Center

Objectives of the study

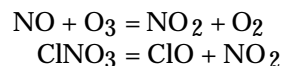
The use of supersonic aircraft with long range and high altitude capabilities has been proposed to obtain atmospheric samples to study the depletion of the ozone layer over the polar regions. However, there is a possibility the samples may change their composition when heated and compressed by the shock waves generated by the supersonic aircraft. The extent of chemical changes which might occur during supersonic sampling will depend on the aircraft speed and altitude and the temperature and pressure history of the sample.

Progress and results

Reacting flow models have been used to determine possible sample chemistry changes due to the increases in temperature and pressure caused by shock waves. The flow environment was calculated along a streamline which began in the undisturbed flow and passed through the shocks before entering the probe. Speeds up to Mach 3 and altitudes to 20 km were covered by the study.

Computational chemistry methods were used to predict thermodynamic properties of important sample species not found in current data bases including heats of formation, specific heats, enthalpy and entropy as functions of temperatures up to 600 K. Reaction mechanisms and thermodynamic data relevant to sample conditions were added to the flow simulations. Conditions after normal or oblique shock were input to the model and parametric studies of sample changes were performed as functions of aircraft speed and altitude. The species of interest in atmospheric sampling include ozone (O_3), oxides of nitrogen (NO , NO_2 , NO_3 , N_2O_5) and chlorine compounds (Cl , ClO , ClO_2 , Cl_2O_2 , $ClNO_3$). Shock heating can convert the species being measured to other compounds. For example, if nitrogen dioxide (NO_2) were

to be sampled, its concentration might be significantly increased from the ambient amount by the following reactions which can occur after shock heating:



The results showed that the chemical integrity of the sample depended on the aircraft speed and the species. For example, at Mach 1, the above reactions do not even occur and the sample is essentially frozen since there are only slight increases in temperature and pressure when bringing the sample to rest. However, at Mach 2, the sample begins to change composition in about 10 milliseconds and at Mach 3, in 1 microsecond. The amount of change which can be tolerated depends on the species being measured and the time required to complete the sample measurements. For example, if the total amount of chlorine is to be measured and individual species data are not needed, then sampling at Mach 3 is possible. If sample speciation is required and the sample heating is too severe to permit chemical integrity, then the possibility exists for sampling from the colder leeward side of a flat plate inclined to the flow. Here, the possibility of ice formation clogging the sampling orifices has to be considered.

Significance of the results

Although there has been speculation about the effects of sampling from supersonic aircraft, there have been no previous studies of this phenomenon. This work combines the unique capabilities of the Computational Chemistry group to predict species' thermodynamic properties and reaction rates with reacting flow modeling to examine this important issue.

The results show that the suitability of supersonic aircraft depends on the sampling requirements. If there is a need for individual species data, then supersonic flight is probably not feasible. However, the measurement of aggregate species, such as chlorine compounds or nitrogen oxides, may be possible.

Keywords

Atmospheric sampling, Ozone depletion, Supersonic flight, Stratospheric chemistry

Organic Matter from H₂O and CO₂ Dissolved in Minerals

Investigator(s)

Narcinda R. Lerner, Ames Research Center,
Moffett Field, CA 94035-1000
Friedemann Freund, San Jose State University
and SETI Institute, Ames Research Center

Other personnel involved

Alka Gupta and Devendra Kumar, SETI Institute,
Ames Research Center
Scott A. Sandford and Max P. Bernstein,
Ames Research Center

Objectives of the study

Formation of complex, stereochemically constrained organic compounds under prebiotic early-Earth conditions is relevant to NASA's Exobiology Program. This study starts from the following independently verifiable premises: 1) the matrix of magmatic minerals represents an unusual reaction medium; 2) when minerals crystallize from H₂O/CO₂-laden magmas, they dissolve H₂O and CO₂; 3) upon cooling, solute H₂O and CO₂ undergo a redox conversion, forming H₂ and reduced carboxy anions; 4) solute H₂ and C segregate to subgrain boundaries and dislocation lines; and 5) as local H₂ and C concentrations increase, H_xC_yO_zⁿ⁻ precursors form at defect sites, stereochemically constrained by the surrounding matrix. These premises lead to the prediction that, when such minerals dissolve during weathering, the lattice-bound H_xC_yO_zⁿ⁻ precursors become H-C-O molecules that will be released into the environment. To test this prediction, extraction and dissolution experiments were conducted under conditions that rigorously controlled contamination, using both synthetic and natural melt-grown minerals. A proof would represent a major step toward a better understanding of the conditions under which life may have arisen on the early Earth about 3.5 billion years ago.

Progress and results

Characterization of the MgO and olivine crystals

Extraction experiments with different organic solvents and dissolution experiments in refluxed water were carried out on coarsely crushed synthetic MgO and natural olivine single crystals, (Mg,Fe)₂SiO₄. The MgO crystals were large, about 5 × 40 mm, grown at 2860°C from a melt produced in a carbon arc fusion furnace, saturated with CO/CO₂/H₂O at 1 bar pressure. The

olivine crystals were 5–20 mm in size, gem-quality transparent or slightly turbid, from San Carlos, Arizona, a locality known for upper mantle rocks brought up by volcanic eruptions. The olivine crystals are known to have grown under high pressures, probably 20–30 Kbars, in a CO₂/H₂O-laden environment.

Soxhlet extractions were performed on 50–100 g of coarsely crushed single crystals. The extractor was thoroughly cleaned and rinsed with deionized water, and subsequently heated to 450°C. Full procedural controls were performed on the thimble without sample and with crushed glass. The samples were extracted sequentially for about 1–24 hours in 100 ml of chloroform, acetone, and tetrahydrofuran (THF) chosen to represent solvents with increasing polarities.

The infrared (IR) absorption spectrum of a double-sided polished olivine crystal from San Carlos, Arizona, shows no features indicating H-C-O molecules. However, it does not rule out the presence of H_xC_yO_zⁿ⁻ precursors having very broad IR bands due to strong coupling to the mineral matrix.

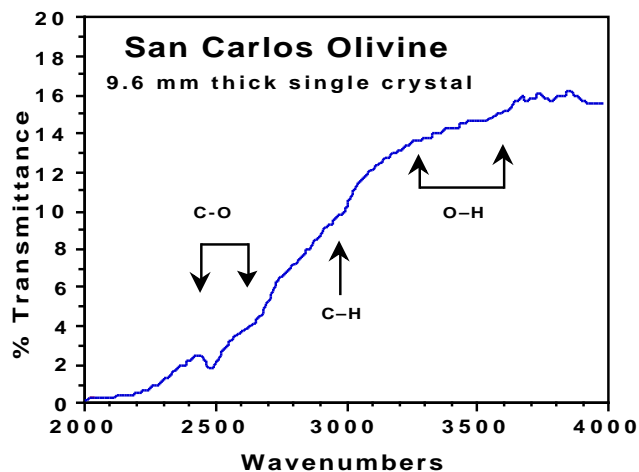


Figure 1. IR absorption spectrum of a thick double-polished section of a San Carlos olivine single crystal. Note the absence of O-H stretching bands between 3300 and 3700 cm⁻¹, the apparent absence of C-H stretching bands around 3000 cm⁻¹, and a broad doublet between 2500 and 2700 cm⁻¹, indicative of C-O bands.

Spectroscopic analysis

The extracts were concentrated. The amount of liquid or solid organic residues obtained was of the order of 10–20 mg. The residues were analyzed by thin-layer chromatography (TLC), infrared (IR), nuclear magnetic

resonance ($^1\text{H-NMR}$), and gas chromatography and mass spectroscopy (GC-MS).

Figures 2 and 3 show the IR spectra of the chloroform and acetone extract residues from the crushed olivine and MgO single crystals, respectively. Samples were prepared by allowing a few drops of the

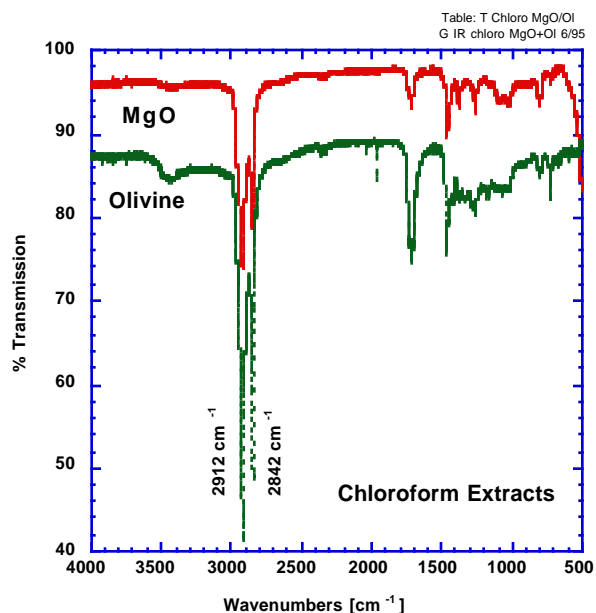


Figure 2. IR spectra: Chloroform extracts.

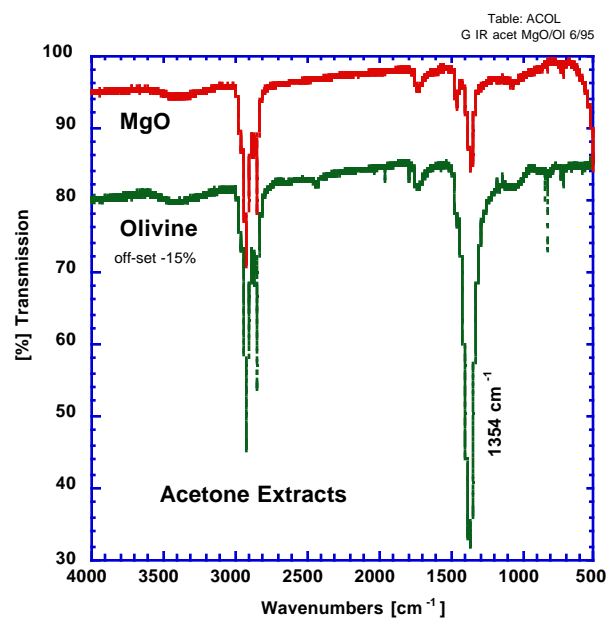


Figure 3. IR spectra: Acetone extracts.

concentrates to dry on a KBr window. The spectra were recorded on a Nicolet 7000 Fourier transform infrared (FT-IR) instrument at Ames. All IR spectra exhibit strong absorption bands near 2912 and 2842 cm^{-1} indicative of C-H stretching bands. The acetone extract gives a strong band at 1354 cm^{-1} . The THF extract gives a strong band at 1723 cm^{-1} , indicative of a carbonyl group, and a broadband between 3000 and 3600 cm^{-1} , indicative of a carboxylic acid group. The IR data are consistent with the presence of $\text{C}_x\text{H}_y\text{O}_n$ -type organic compounds.

The $^1\text{H-NMR}$ spectra were recorded with a Bruker NMR spectrometer. The chloroform extract shows aliphatic methyl and methylene groups. The hyper-splitting observed near 4–5 ppm suggests heteroatom or olefinic protons. No signal was observed in the aromatic region. The acetone extract shows methyl and methylene groups as singlets. The absence of coupling means that these groups are either separated by a heteroatom or a C atom carrying no protons. The THF extract gives a complex $^1\text{H-NMR}$ spectrum, indicating the presence of aliphatic methyl and methylene groups.

GC-MS analyses were performed on a Hewlett Packard 5971 instrument equipped with a capillary column and a data station. The chloroform extract from olivine shows a GC elution peak at 8.14 min, with a mass spectrum characteristic of an aliphatic hydrocarbon chain as evidenced by CH_2 increments. A fragment at 43 atomic mass units (amu) along with incremental fragments, separated by 14 amu, indicates a series of alkyl ions ($\text{C}_n\text{H}_{2n+1}^+$). The 73 and 87 amu fragments suggest oxygen. A fragment at 41 amu with 14 amu increments and an 153 amu fragment are indications of a $\text{CH}_2 = \text{CH}$ -terminated C-11 alkyl chain. This is complemented by the $^1\text{H-NMR}$ spectrum showing a strong methylene (CH_2) singlet at 1.25 ppm with a methyl (CH_3) singlet, and by the IR spectra showing C-H stretching bands at 2912 and 2842 cm^{-1} . The GC peak eluted at 12.33 min of the chloroform extract shows a base peak at 71 amu, suggesting the presence of a $\text{CH}_3\text{CH}_2\text{CH}(\text{CH}_3)_2^+$ fragment.

Significance of the results

According to the results obtained in this study, the premises on which the starting hypothesis was based appear to be correct. Undoubtedly, organic compounds can be extracted from crushed olivine single crystals that originated in the $\text{CO}_2/\text{H}_2\text{O}$ -laden, high-pressure environment of the upper mantle. Likewise, similar organic compounds can be extracted from melt-grown synthetic MgO crystals, though the work to identify these compounds is still in progress and

needs to be expanded to include dissolution experiments simulating weathering of rocks on the early Earth.

If the complex organic compounds extracted from olivine indeed derive from H_2O and CO_2 structurally dissolved in these upper mantle crystals, as the data suggest, the present observation would have far-

reaching consequences for better understanding the natural conditions under which life arose.

Keywords

Origin of life, Abiogenic synthesis, Extraction of organics

The Opacity of Water Vapor

Investigator(s)

Harry Partridge and David Schwenke,
Ames Research Center,
Moffett Field, CA 94035-1000

Objectives of the study

To determine accurate opacities for hot water vapor, which are required for modeling the atmospheres of oxygen-rich cool evolved stars (CES). The relatively low surface temperature of these stars results in a high concentration of molecular species in their atmospheres, and the spectra of these stars are dominated by many overlapping molecular bands. Considerable effort has been devoted to constructing model atmospheres of CES, but progress is limited by the lack of accurate opacities for water vapor at stellar temperatures. The available laboratory data are insufficient to accurately specify the opacities. However, the required opacity data can be obtained by quantum mechanical calculations that solve both the electronic and the nuclear Schrodinger equations. This project involves three principal steps: 1) determination of an accurate dipole moment surface for water; 2) development of a hybrid potential energy surface for water using the accurate experimental potential near the equilibrium geometry and the ab initio results for highly distorted geometries; and 3) determination of the ro-vibrational energy levels and their intensities for all levels that are significantly populated at stellar temperatures.

Progress and results

The ab initio electronic structure calculations to determine the dipole moment and potential energy surfaces have been completed; approximately 600 geometries were needed to represent the surfaces. The computed energy surface is in excellent agreement with the experimentally derived surface up to about $20,000\text{ cm}^{-1}$, which represents the energy regions for which spectroscopic data are available. At energies in the region $25,000$ to $40,000\text{ cm}^{-1}$, substantial errors are obtained by simply extrapolating the experimental potential.

The ab initio data were used to define a preliminary potential energy surface (PES1). This surface was then adjusted by varying the six lowest-order expansion parameters and adding three extra kinetic energy parameters (to approximately correct for electronic

nonadiabaticity); the resulting surface is called PES2. The nine parameters in PES2 were determined by matching the line positions of the experimental Q(1) branch using nonlinear weighted least squares. This adjustment took the unweighted root-mean-square (rms) error down from 6.94 cm^{-1} to 0.12 cm^{-1} .

Then PES2 was used to solve for the ro-vibrational wavefunctions for high vibrational levels and total angular momenta 0 to 42. This converges the partition function for temperatures up to about 3000 K. The ro-vibrational wavefunctions were computed using the Rayleigh—Ritz variational principle, and all vibrational and rotational coordinates were coupled. The only approximations involved in the ro-vibrational calculations were the use of a finite basis set expansion and numerical quadratures. The ro-vibrational calculations used hyperspherical Radau coordinates. The ro-vibrational wavefunctions along with the ab initio dipole moment function were then used to compute the line strengths. A total of 5,639,020 lines were generated. Calculations were carried out only for the $^1\text{H}^1\text{H}^{16}\text{O}$ isotope of water.

Significance of the results

The computed potential energy surface has been shown to agree with the experimentally derived surface in regions where the experimental potential is well defined. This gives confidence that the computed dipole and energy surfaces are accurate. Detailed comparisons of the results obtained using PES2 and the results from other currently available potentials show that PES2 gives a much more uniform description of the vibrations in water. The description of rotation by PES2 is not quite as good as one other potential in the literature, but this seems to be due to cancellations of error, since the principal deficiency of PES2 is an incomplete treatment of electronic nonadiabaticity. Thus the line strength data generated by PES2 should be significantly more accurate than results obtained using other surfaces. Further refinement of PES2 is possible, but PES2 is already accurate enough to show that some of the lines from experiment (the HITRAN database) have been incorrectly labeled. This makes refinements based on experimental data risky, because one may be trying to fit to the wrong lines. Additional electronic structure calculations of nonadiabatic coupling terms will probably be the only sure way to improve PES2.

Publications resulting from study

The water line list has not been published, but it is available from the authors. The citation to the line list should be “Water opacity data of David W. Schwenke and Harry Partridge, June 1995, unpublished.”

Keywords

Water opacity, Dipole moment surface, Ro-vibrational wavefunctions

Deep Near-Infrared Cosmological Surveys

Investigator(s)

Thomas L. Roellig and Edwin F. Erickson,
Ames Research Center,
Moffett Field, CA 94035-1000
Jacqueline A. Davidson, SETI Institute,
Ames Research Center

Other personnel involved

Arati Chokshi, California Institute of Technology,
Pasadena, CA 91125

Objectives of the study

Deep-sky imaging of fields of distant galaxies can serve as an excellent probe of the space-time curvature of the universe if galaxies are uniformly distributed throughout space on a sufficiently large scale. If space is curved, then measuring the number density of galaxies as a function of distance can serve as a measure of the curvature. Therefore, measurements of distant galaxies can help answer one of the most important questions in cosmology: whether the universe is open and will continue expanding forever, or closed, in which case it will eventually stop expanding and instead collapse again in a “Big-Crunch.” This concept is shown in figure 1, which shows the difference in the cumulative number of galaxies counted vs. red shift in open ($\Omega = 0$) and closed ($\Omega = 1$) universes. These measurements can also set strong constraints on the existence of the various exotic particles (such as WIMPS, MACHOS, etc.) that have been postulated to be responsible for the missing mass in the universe. It

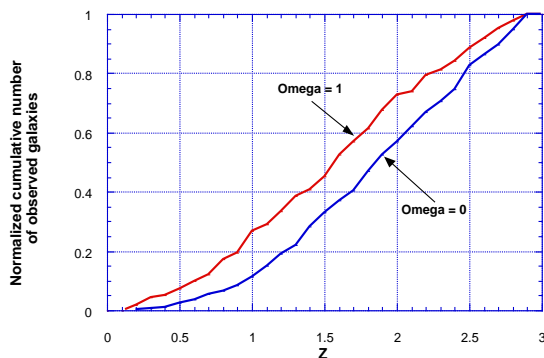


Figure 1. The cumulative number of galaxies vs. red shift for $\Omega = 0$ and $\Omega = 1$ universes, each normalized to 1. This shows that there is a clear observable difference between the cosmologies, even without using absolute galaxy number counts.

is possible to use near-infrared (NIR) images taken at a number of wavelengths to determine the number density vs. distance relationship for galaxies. The present objective is to determine the envelope of parameters within which NIR imaging surveys with a small dedicated space mission will have the maximum impact on cosmology studies.

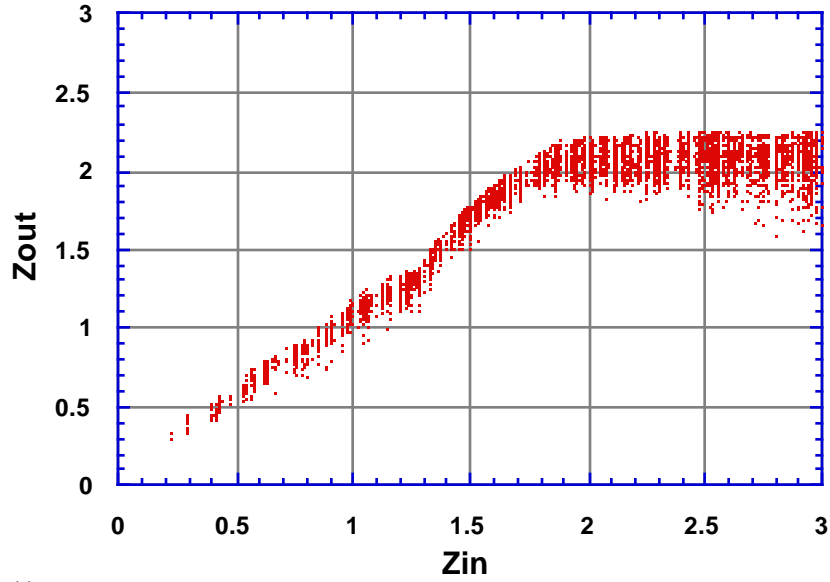
Progress and results

In the course of this study, a detailed model of galaxies as they would appear in both closed and open universes has been generated. This model accurately depicts the appearance of the spectra of spiral, elliptical, and irregular galaxies in the 1–10 μm wavelength range out to red shifts of 3.0. The model shows that galaxies of all types have a peak in their NIR energy distribution located at $\sim 1.6 \mu\text{m}$. In distant galaxies, this peak will be red shifted to longer wavelengths. Using NIR measurements, this red shift can be estimated and the red shift/distance relationship can then be used to calculate number densities. Results indicate that, in order to discriminate between open and closed universes, such observations would require: 1) good sensitivity; 2) sensitivity to wavelengths longer than 5 μm to be able to measure the red shift of galaxies with red shift z greater than ~ 1.5 ; 3) sampling at wavelengths spaced no more than 1 μm apart in order to eliminate excess noise in the total number N vs. z plots; and 4) very accurate estimates of galaxy merger rates. As an example, figures 2(a) and (b) indicate that observations limited to wavelengths less than 5 μm will not give accurate red shifts beyond 1.7.

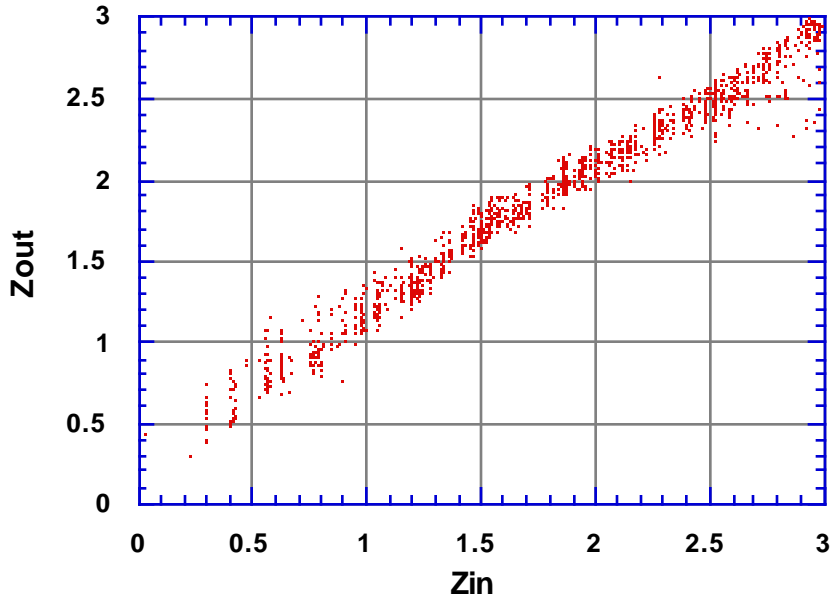
The results of this study can now be used to design a dedicated space mission to make the required observations. Going to space is necessary to get above the Earth’s atmosphere and its absorption in the critical 5–10 μm spectral region. In addition, the vacuum of space will allow the telescope optics to be cooled by either active or passive means, allowing enormously higher sensitivities at the longer infrared wavelengths than is possible from ground-based or airborne telescopes operating at ambient temperatures. Such a mission could easily fit within the constraints of the midsized explorer (MIDEX) program and, with careful design, could possibly also fit within the small explorer (SMEX) program.

Keywords

Cosmology, Near-infrared imaging, Source-counts



(a)



(b)

Figure 2. Plots of the derived red shifts (Z_{out}) of the model galaxy population at various true red shifts (Z_{in}). In the case of figure 2(a), Z_{out} was determined by samples at $1\text{-}\mu\text{m}$ intervals from 1 to $5\ \mu\text{m}$. In the case of figure 2(b), Z_{out} was determined by samples at $1\text{-}\mu\text{m}$ intervals from 1 to $10\ \mu\text{m}$. These plots indicate that observations at wavelengths longer than $5\ \mu\text{m}$ are needed if accurate derivations of red shifts greater than ~ 1.7 are to be made.

Does the Collapse of Diatom Blooms Trigger Coccolithophore Blooms?

Investigator(s)

Lynn Rothschild,
Ames Research Center,
Moffett Field, CA 94035-1000

Objectives of the study

The determination of global carbon fluxes is a pressing concern for climatic, and thus economic, medical, and political reasons. A particularly important player in marine carbon fluxes is the coccolithophores, a group of planktonic algae that fix CO₂ into organic matter as well as deposit carbonate in coccoliths, plates that cover the cell. Coccolithophores are a significant carbon sink (ref. 1), although they may sometimes also be a source of CO₂ (ref. 2). Coccolithophores are also important because they are linked to the global sulfur cycle as major producers of dimethyl sulfide, a gas that may moderate global temperatures (refs. 3 and 4).

Emiliana huxleyi is by far the most abundant and widespread coccolithophore, ranging from the Arctic to Antarctic convergences (refs. 5 and 6). This species forms huge blooms which, because of the coccoliths, are easily detected by remote sensing. The blooms are important in sequestering inorganic carbon. For example, a 7200-km² bloom between France and Ireland contained an estimated 7.2×10^4 tons of calcite (ref. 7).

The blooms are an annual early summer event, but the triggers of these massive blooms is unknown. Possible causes include water mixing and elevated nutrient levels (refs. 8 and 9). More intriguing is the fact that *E. huxleyi* blooms typically follow the collapse of early spring diatom blooms. The question: "Is there a causal relationship between the collapse of the diatom blooms and the onset of the *Emiliana* blooms?" is addressed in this study. Alternatively, it could be coincidental or caused by the preference of *Emiliana*

for warmer water or higher solar irradiance. The immediate objective is to determine if there is a causal relationship between the end of a diatom bloom and the beginning of an *Emiliana* bloom, and if so, what its chemical basis is. The ultimate objective is to predict the onset of *Emiliana* blooms to better monitor them by remote sensing. The data may suggest ways to alter the global carbon cycle by triggering or suppressing *Emiliana* blooms.

Progress and results

The growth rates and biomasses of *E. huxleyi* grown in both natural seawater and seawater that was preconditioned with a culture of bloom-forming diatoms were compared to determine if the collapse of diatom blooms could trigger *Emiliana* blooms. The seawater was obtained from the Pacific Ocean off the shore in Santa Cruz, California, and the water was sterilized by autoclaving. Portions of the water were inoculated with one of several species of common marine diatoms (table 1). After the culture grew to stationary phase, as monitored by phase-contrast microscopy, the water was filtered with a 0.2- μ m filter to remove all living organisms. The treated and untreated seawaters were inoculated with a calcifying strain of *Emiliana huxleyi* (table 1). Cell counts were made every few days using a hemocytometer. All experiments were performed in replicate (n = 2-6).

The results clearly indicate that the diatoms alter the seawater in some way that enhances the growth of the *Emiliana* (fig. 1). This supports the hypothesis that the diatoms in some way trigger *Emiliana* blooms.

If the collapse of diatom blooms triggers *Emiliana* blooms, what could be the nature of the causal relationship? Diatom blooms may collapse from nitrate, silicate, or iron limitation (refs. 9 and 10). Unlike diatoms, coccolithophores do not

Table 1. Cultures and their sources

Culture	Source
<i>Skeletonema costatum</i>	Gulf of Mexico (UTEX LB 2308)
<i>Thalassiosira sp.</i>	Singapore (UTEX LB 2054)
<i>Phaeodactylum sp.</i>	Pacific Ocean
<i>Emiliana huxleyi</i>	Gulf of Maine (CCMP 374)

utilize silicate, so silicate limitation should not affect coccolithophore blooms. Low nitrate or iron might enhance *Emiliana* growth, but what the mechanism might be is unclear. There is some evidence that in a bloom, phosphate concentration $>0.5 \mu\text{M}$ lowers calcification (ref. 9) and *Emiliana* grows better in low phosphate waters than competing phytoplankton (ref. 11), so lower levels of phosphate may trigger a bloom. After the collapse of a diatom bloom, surface-water levels of dissolved inorganic carbon (DIC) may be severely depleted (ref. 12). Laboratory experiments on blue-green algae, phytoplankton, and marine macroalgae (refs. 1 and 13–19), indicate that many photosynthetic protists may be carbon limited under ambient conditions. Short-term field studies on carbon fixation in algal mats (refs. 20–22) and long-term field studies on wetland grasses (ref. 23) support the concept of carbon limitation in nature. However, carbon metabolism in *E. huxleyi* is complex. In photosynthesis, CO_2 enters the cell and is used in the chloroplast to produce organic carbon (refs. 24–26). Inorganic carbon also enters the cell as HCO_3^- , which is deposited as coccolith carbonate (ref. 8). Carbon dioxide and water that evolves during carbonate deposition can be used in photosynthesis, although some may be released and ventilated to the atmosphere (refs. 2 and 27). The fact that *E. huxleyi* produces CO_2 as a byproduct of calcification may allow it to grow in the DIC-depleted waters (ref. 10). In contrast, the initial experiments on *Emiliana huxleyi* (ref. 28) showed that growth rates at pH 8.0 are significantly increased by inorganic carbon in excess of average seawater values of $\sim 2 \mu\text{M}$, a result consistent with that of reference 29.

Previous to this work, a consensus was emerging in the community that the *Emiliana* were at a competitive advantage after the collapse of a diatom bloom because the water would be depleted in free CO_2 , but the *Emiliana* could produce CO_2 from HCO_3^- by calcification. The results of this study suggest a more direct effect. Interestingly, research (ref. 30) has shown that diatoms excrete thiamine, and that *Emiliana* need thiamine for growth. This suggests a direct chemical mechanism to explain the results of this study.

Significance of the results

This work will be significant for the prediction of *Emiliana* blooms and for the improved use of satellite imagery in monitoring blooms. Results suggest that thiamine levels or diatom concentrations can

be used to predict or manipulate the onset of *Emiliana* blooms. If we understand what triggers blooms, we will have the power to alter global carbon fluxes by preventing or enhancing blooms. This is particularly meaningful in light of rising levels of atmospheric CO_2 .

References

1. Sikes, C. S.; and Fabry, V. J.: Regulation of Atmospheric CO_2 and O_2 by Photosynthetic Carbon Metabolism. In Photosynthetic Carbon Metabolism and Regulation of Atmospheric CO_2 and O_2 , N. E. Tolbert and J. Preiss, eds., Oxford Press, Oxford, 1994, pp. 217–233.
2. Holligan, P. M.; and Balch, W. M.: From the Ocean to Cells: Coccolithophore Optics and Biogeochemistry. In Particle Analysis in Oceanography, S. Demers, ed., Springer Verlag, Berlin, 1991, pp. 301–324.
3. Keller, M. D.; Bellows, W. K.; and Guillard, R. R. L.: The Importance of Species Specificity in the Production of Dimethylsulfide by Marine Phytoplankton. In Biogenic Sulfur in the Environment, ACS Symposium Series, E. Salzman, ed., vol. 393, ACS Books, 1989, Washington, D.C., pp. 167–182.
4. Schlesinger, W. H.: Biogeochemistry, An Analysis of Global Change. Academic Press, San Diego, 1991.
5. McIntyre, A.; and Bé, A. W. H.: Modern Coccolithophoridae of the Atlantic Ocean—1. Placoliths and Cyrtoliths. Deep Sea Res., vol. 14, 1967, pp. 561–597.
6. Okada, H.; and Honjo, S.: The Distribution of Oceanic Coccolithophorids in the Pacific. Deep-Sea Research and Oceanographic Abstracts, vol. 20, no. 4, 1973, pp. 355–374.
7. Holligan, P. M.; Viollier, M.; Harbour, D. S.; Camus, P.; and Champagne-Philippe, M.: Satellite and Ship Studies of Coccolithophore Production along a Continental Shelf Edge. Nature, vol. 304, 1983, July 28, 1983, pp. 339–342.
8. Westbroek, P.; Young, J. R.; and Linschooten, K.: Coccolith Production Biomineralization in the Marine Alga. J. Protozool., vol. 36, no. 4, 1989, pp. 368–373.
9. Balch, W. M.; Holligan, P. M.; Ackleson, S. G.; and Voss, K. J.: Biological and Optical Properties of Mesoscale Coccolithophore Blooms in the Gulf of Maine North Atlantic Ocean. Limnol. Oceanogr., vol. 36, no. 4, 1991, pp. 629–643.

10. Westbroek, P.; van Hinte, J. E.; Brummer, G.-J.; Veldhuis, M.; Brownlee, C.; Harris, R.; and Heimdal, B. R.: The Coccolithophore *Emiliana huxleyi* and Global Climate. *Bio-Japan* 1992, pp. 255–263.
11. Egge, J. K.; and Heimdal, B. R.: Blooms of Phytoplankton including *Emiliana huxleyi* (Haptophyta): Effects of Nutrient Supply in Different N:P Ratios. *Sarsia*, vol. 79, no. 4, 1994, pp. 333–348.
12. Riebesell, U.; Wolf–Gladrow, D. A.; and Smetacek, V.: Carbon Dioxide Limitation of Marine Phytoplankton Growth Rates. *Nature*, vol. 361, 1993, pp. 249–251.
13. Badger, M. R.; and Andrews, T. J.: Photosynthesis and Inorganic Carbon Usage by the Marine Cyanobacterium, *Synechococcus sp.* *Plant Physiol.*, vol. 70, 1982, pp. 517–523.
14. Brechignac, François; and Andre, Marcel: Oxygen Uptake and Photosynthesis of the Red Macroalga, *Chondrus crispus*, in Seawater. *Plant Physiol.*, vol. 75, 1984, pp. 919–923.
15. Beer, S.; and Shragge, B.: Photosynthetic Carbon Metabolism in *Enteromorpha Compressa* (Chlorophyta). *J. Phycol.*, vol. 23, 1987, pp. 580–584.
16. Holbrook, G. P.; Bier, S.; Spencer, W. E.; Reiskind, J. B.; Davis, J. S.; Bowes, G.: Photosynthesis in Marine Macroalgae Evidence for Carbon Limitation. *Can. J. Bot.*, vol. 66, no. 3, 1988, pp. 577–582.
17. Reiskind, J. B.; Seamon, P. T.; and Bowes, G.: Photosynthetic Responses and Anatomical Features of Two Marine Macroalgae with Different Carbon Dioxide Compensation Points. *Aquatic Botany*, vol. 33, no. 1–2, 1989, pp. 71–86.
18. Gao, K.; Aruga, Y.; Asada, K.; Ishihara, T.; Akano, T.; and Kiyohara, M.: Enhanced Growth of the Red Alga *Porphyra yezoensis ueda* in High CO₂ Concentrations. *J. Appl. Phycol.*, vol. 3, 1991, pp. 355–362.
19. Levavasseur, G.; Edwards, G. E.; Osmond, C. B.; and Ramus, J.: Inorganic Carbon Limitation of Photosynthesis in *Ulva Rotundata* (Chlorophyta). *J. Phycol.*, vol. 27, 1991, pp. 667–672.
20. Rothschild, Lynn J.; and Mancinelli, Rocco L.: Model of Carbon Fixation in Microbial Mats from 3,500 Myr Ago to the Present. *Nature*, vol. 345, June 21, 1990, pp. 710–712.
21. Rothschild, L. J.: Elevated CO₂: Impact on Diurnal Patterns of Photosynthesis in Natural Microbial Ecosystems. *Adv. Space Res.*, vol. 14, no. 11, 1994, pp. 285–289.
22. Rothschild, L. J.: CO₂ and Diatom Mats. *Nature*, vol. 368, 1994, p. 817.
23. Drake, B. G.: A Field Study of the Effects of Elevated CO₂ on Ecosystem Processes in the Chesapeake Bay Wetland. *Aust. J. Bot.*, vol. 40, 1992, pp. 579–595.
24. Sikes, C. S.; Roer, R. D.; and Wilbur, K. M.: Photosynthesis and Coccolith Formation Inorganic Carbon Sources and Net Inorganic Reaction of Deposition. *Limnology and Oceanography*, vol. 25, no. 2, 1980, pp. 248–261.
25. Nimer, N. A.; Dixon, G. K.; and Merrett, M. J.: Utilization of Inorganic Carbon by the Coccolithophorid *Emiliana–huxleyi* Lohmann Kamptner. *New Phytologist*, vol. 120, no. 1, 1992, pp. 153–158.
26. Nimer, N. A.; and Merrett, M. J.: Calcification and Utilization of Inorganic Carbon by the Coccolithophorid *Emiliana–huxleyi* Lohmann Kamptner. *New Phytologist*, vol. 121, no. 2, 1992, pp. 173–177.
27. Purdie, D. A.; and Finch, M.: The Impact of *Emiliana huxleyi* Blooms on pCO₂ in Coastal Waters: Preliminary Results from Mesocosm Experiments. Abstract presented at “The Biology of the Prymnesiophyta” (an international symposium held at The University of Plymouth, Mar. 29–Apr. 1, 1993).
28. Rothschild, L. J.; and Squire, B. T.: The Relationship between Growth Rate and Carbon Fixation under Elevated Levels of Inorganic Carbon in *Emiliana huxleyi*. *J. Euk. Microbiol.*, vol. 42, 1995, p. 42A.
29. Sikes, C. S.; and Wilbur, K. M.: Calcification by Coccolithophorides: Effects of pH and Sr. *J. Phycol.*, vol. 16, 1980, pp. 433–436.
30. Carlucci, A. F.; and Bowes, P. M.: Production of Vitamin B₁₂, Thiamine, and Biotin by Phytoplankton. *J. Phycology*, vol. 6, no. 4, 1970, pp. 351–357.

Keywords

Emiliana, Phytoplankton blooms, Global change

Improving Future Space Missions by Capitalizing on Aeropass Maneuvers of the Magellan Spacecraft

Investigator(s)

Paul Wercinski, Ames Research Center,
Moffett Field, CA 94035-1000
Brian Haas, Thermosciences Institute,
Ames Research Center

Other personnel involved

Robert Tolson, George Washington University,
Washington, DC 20052

Objectives of the study

An innovative experiment involving repeated aeropasses of the Magellan spacecraft in orbit around Venus has generated valuable flight data that have been used to improve gas-surface interaction (GSI) models and explore aeropass maneuver scenarios for future planetary missions. The Magellan “Windmill” experiment was conducted in the autumn of 1994; it involved canting the spacecraft solar panels during atmospheric aeropasses to induce aerodynamic torques on the spacecraft as a result of gas-surface mechanics. The proposed research simulated Magellan’s aeropass maneuvers computationally to deduce GSI coefficients from the spacecraft response data. The objectives of this study were to characterize GSI phenomena in the context of orbital aeropass maneuvers. This included quantifying parameters in current GSI engineering models and assessing sensitivities to surface normal direction, surface material, gas species, and flow rarefaction. An additional objective was to assess the use of aerobraking for future missions.

Progress and results

At each aeropass flight condition during a periapsis passage, the spacecraft configuration and attitude were known. Reaction wheels compensated for aerodynamic torques to maintain a predetermined spacecraft attitude. Interpreting the reaction wheel data enabled a measurement of the transient torques acting on the spacecraft. The torques measured about the roll axis (y-axis) are exclusively dependent upon particle reflection from the solar panels and are independent of the bulk free-stream momentum flux. A diagram of the Magellan spacecraft is shown in figure 1. Using flight data, the variation of torques (M_x , M_y , M_z) as functions of time has been resolved.

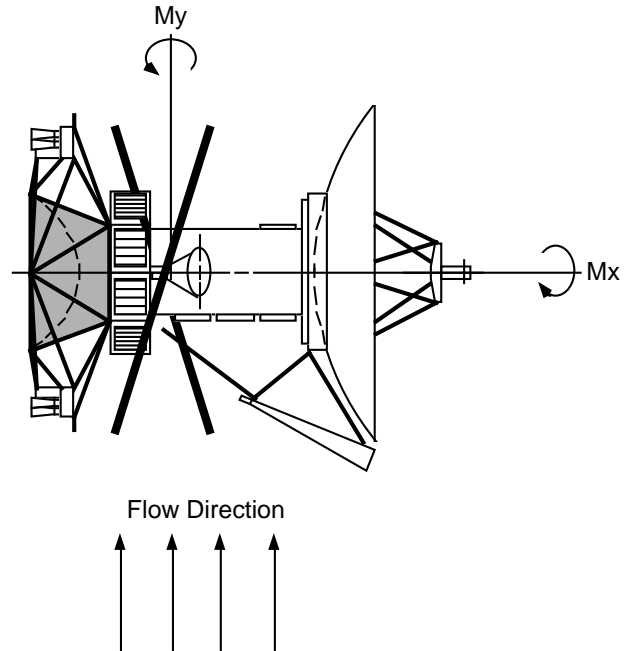


Figure 1. Magellan spacecraft in windmill configuration.

The spacecraft dynamics at periapsis have been the current focus of the analysis since this represents the conditions of maximum forces acting on the spacecraft and thus yields data with the highest signal-to-noise ratio. In order to reduce the unknown variables in the analysis, ratios of moment coefficients (M_y/M_x , M_z/M_x) were determined at periapsis for a number of orbit passages. Using a computational code called FMAC, a set of unique normal and tangential accommodation coefficients (σ_t and σ_n) for the Magellan spacecraft attitude, geometry, and flight conditions was calculated. A relationship of the moment ratios that determine a unique set of accommodation coefficients was determined. Furthermore, the set of accommodation coefficients is a function also of the relative angle of attack of the solar panels to the spacecraft velocity vector.

As a result of close inspection of the flight data and the corresponding simulations, the M_z data were found to be very noisy because the data were very small in magnitude in comparison to the other moment values about the x- and y-axes. In contrast, the M_y data were found to be predictable and much less noisy. The M_y/M_x data can thus be used as a

valuable constraint on the variation of σ_t and σ_n as functions of local angle of attack. Figure 2 shows the estimated variations of σ_t and σ_n for several angles of attack as determined from the M_y/M_x data. Unfortunately, the accommodation coefficients cannot be fully determined without another independent constraint. This complication to the analysis process was not expected and thus significantly increased the time and effort needed to resolve a verifiable accommodation coefficient relationship.

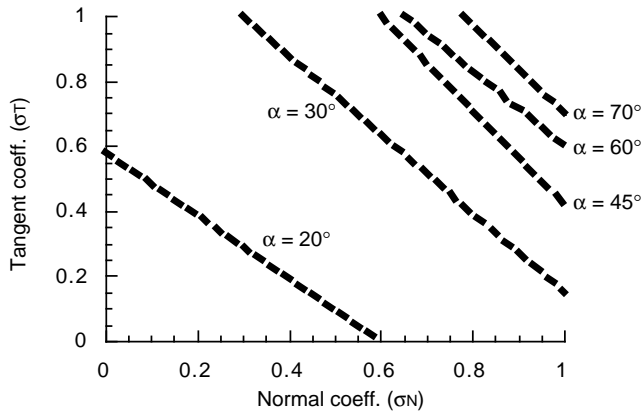


Figure 2. Surface accommodation coefficient variations at different solar panel angles of attack from M_y/M_x data.

The analytic procedure for providing the needed second constraint involves integrating the aeropass flight trajectory with a simulation code that will estimate the spacecraft drag coefficient variation through

the atmosphere passage. The simulation will further “loop” through a range of σ_t and σ_n such as to arrive at an effective average value of σ_t and σ_n , which yields a good reconstruction of the actual flight trajectory. The appropriate values of σ_t and σ_n determined from the trajectory reconstruction can then be coupled with the values of σ_t and σ_n determined from the M_y/M_x FMAC simulations to yield a unique set of σ_t and σ_n to satisfy both constraints. This analysis effort has not yet been completed.

Significance of the results

The determination of surface accommodation coefficients for spacecraft flying in rarefied flow conditions has remained one of the great unknowns since the conditions of velocity, atmosphere species composition, and density cannot be modeled in ground facilities. For the effort initiated in this research, the two independent constraining conditions, the relationships of normal and tangential surface accommodation coefficients, can be constructed as functions of local angle of attack. These values of σ_t and σ_n can then be used to verify the model predictions with the actual flight data from the Magellan spacecraft. The improved values of σ_t and σ_n can then be used in GSI models such as the Hurlbut–Sherman–Nocilla reflection model. With this improved modeling capability, future predictions of rarefied gas-flow interactions on orbiting spacecraft for future space missions can be carried out with greater precision.

Keywords

Gas-surface interaction, Aeropass, Magellan spacecraft

Orbiting Infrared Spectral Flux Calibrators

Investigator(s)

Eliot Young and Fred Witteborn,
Ames Research Center,
Moffett Field, CA 94035-1000

Objectives of the study

The orbiting infrared (IR) spectral flux calibrator is intended to establish a network of stars and asteroids as IR flux standards. Current IR standards may be as good as 5 percent over the 3–30 micron range. In general, it is exceedingly difficult to achieve even 10-percent accuracy over that range. The present objective is to launch a large, inflatable satellite to act as a temporary standard.

Progress and results

The proposed satellite would appear as a star to a ground-based observer, albeit one with very well-known spectra. It would provide an order of magni-

tude improvement in the calibration of other stars and asteroids over a wavelength regime that is useful for understanding composition and temperature of celestial objects. Table 1 gives the characteristics of the proposed satellite.

Two partners have been involved in this endeavor: the Stanford Satellite Development Laboratory and L'Garde, Inc. L'Garde has over 20 years of experience in developing inflatable spacecraft and components. Their 15-meter inflatable parabolic reflector will be tested on an upcoming Shuttle mission (currently scheduled for May 1996). The Stanford group has been building very small, inexpensive satellites at a cost of approximately \$50,000 per satellite. The present study can take advantage of the work they have done in developing a small, robust platform, solar-cell power system, and communications system.

Keywords

Inflatable, Satellite, Calibration, Standard

Table 1. Proposed balloon characteristics

Size	100 ft diameter (angular diameter of 0.15 arcseconds)
Material	Orcon or aluminized mylar
Internal pressure	Approx. 10^{-5} atm.
Launch weight	Less than 100 kg
Orbit	Near geosynchronous or geo-transfer
Surface temperature	380–400 K
Flux	Over 300 J at the blackbody peak (around 14 μm)

SECTION 2
ONGOING REPORTS

Waterproofing the Space Shuttle Tiles

Investigator(s)

Charles W. Bauschlicher, Jr.,
Ames Research Center,
Moffett Field, CA 94035-1000

Objectives of the study

The Space Shuttle tiles are composed of silica, but they contain more than 90 percent empty space. Whereas the pure silica is hydrophobic, if exposed to water surface OH groups form on the surface. These surface OH groups change the silica from hydrophobic to hydrophilic. This change means that the surface now wets, and capillary action will fill the empty space in the tiles with water. This increases the tile's weight, and, perhaps more importantly, degrades the thermal protection properties of the tiles. To avoid this problem the tiles are treated with a waterproofing agent, but unfortunately, the heat of reentry eliminates the waterproofing agent. Thus after each flight, each tile must be injected with a new waterproofing agent. The objective of this study is to find a modification to the silica surface to make it permanently hydrophobic.

Progress and results

A series of calibration calculations was performed to determine the level of theory required to study the interaction of molecules with the silica surface. The relative binding energy of water to pure silica and silica-OH surfaces was compared with that for water, and was used to explain why the silica-OH wets while pure silica does not, in spite of the fact that water was observed in the infrared spectra of both surfaces. The silica-OH binding energy was found to

be slightly smaller than the silica-F and larger than the silica-Cl binding energy. This is consistent with experiment that shows that F is slowly displaced by OH, while Cl is rapidly displaced. The factory waterproofing agent was found to have about the same binding energy as F. This suggests that both the thermodynamics of the water displacement reaction and the umbrella effect make this an effective waterproofing agent.

The binding energies of a series of compounds was computed and compared to the OH binding energy. The only compounds that appeared to offer the possibility of permanent waterproofing were the early transition metal fluorides. These systems have a very strong metal-F bond because of F lone-pair donation into the empty metal 3d orbitals. They also have high melting points. These systems were suggested for experimental study.

Alumina surfaces are being compared with silica surfaces. The calculations suggest that it is harder to waterproof alumina because the surface-OH bond is stronger relative to the other surface-X bonds when compared with silica.

Significance of the results

If the proposed transition metal fluorides make the tiles permanently waterproof, the maintenance costs associated with the Space Shuttle and future reusable space vehicles will be dramatically reduced. In addition, the calculations are helping the understanding of the current experimental work.

Keywords

Waterproofing, Thermal protection, Surface chemistry

Thermal Protection Systems for Reusable Vehicles

Investigator(s)

Jeffrey V. Bowles, Ames Research Center,
Moffett Field, CA 94035-1000
Henry Adelman, Thermosciences Institute,
Ames Research Center

Other personnel involved

Mark Loomis, Sterling Software,
Ames Research Center

Objectives of the study

Demonstration of coupled trajectory/thermal protection system (TPS) concept optimization for minimum TPS system weight integrated on reusable launch vehicle. The study approach involves the use of

an existing hypersonic vehicle synthesis code, and the effort will focus on enhancements to that code for higher fidelity heat transfer and trajectory calculations.

Progress and results

The first year effort will focus on the upgrade and enhancement method of predicting heat transfer for re-entry vehicles as modeled by the conceptual design code. Development of the trajectory optimization method coupled to TPS sizing calculations will then be addressed.

Keywords

Thermal protection system, Re-entry trajectory optimization, Reusable launch vehicle

Planar Interferometric Measurement of Skin Friction

Investigators

James L. Brown and Jonathan Naughton
Ames Research Center,
Moffett Field, CA 94035-1000

Objectives of the study

To develop an instrument to measure the two components, t_x and t_z , of the wall skin friction generated by three-dimensional (3-D) aerodynamic flows. The instrument is based on run-time optical imaging of fringes formed within a thin film of oil placed on the test wall surface that responds to the applied 3-D flow. Data analysis involves an inverse solution of the 3-D thin-oil-film equations. Extensive regions of a test surface are measured by this technique in a single wind-tunnel run. Enhanced wind-tunnel productivity will result as a consequence of the new instrument.

Progress and results

During the previous fiscal year (FY), the instrument setup concept was determined, the component technologies required for implementation of the instrument package were examined, and key equipment, including the framegrabber, image processing hardware, and optical hardware, was purchased. Image processing algorithms and an "inverse" thin-oil-film solution algorithm were developed to derive the wall shear stress from the instrument measurement. During

the next FY, assembly of the prototype instrument will be completed, development of the software package will be completed, and the completed prototype instrument will be applied to a 3-D aerodynamic flow in order to validate the instrument package. Then the software package and equipment and procedure specifications will be released for technology transfer.

Significance of the results

Wall skin friction accounts for about one-half of the drag of an aircraft at cruise conditions. Because of past difficulties in measuring the wall skin friction, wind-tunnel testing typically does not include these important measurements. Inclusion of these measurements with a time-efficient and accurate instrument will considerably enhance the value of wind-tunnel data produced.

Publications resulting from study

Brown, James L.; and Naughton, Jonathan: Planar Interferometric Measurement of Skin Friction. Abstract submitted to 19th AIAA Advanced Measurement and Groundbased Testing Conference, New Orleans, La., June 18-21, 1996.

Keywords

Skin friction, Three-dimensional, Turbulent boundary layers

Computer Modeling of the Thermal Conductivity of Cometary Ice

Investigator(s)

Theodore E. Bunch, Michael A. Wilson, and Andrew Pohorille, Ames Research Center, Moffett Field, CA 94035-1000

Objectives of the study

1. To generate samples of amorphous water ices at different microporosities.
2. To compare the resulting molecular structure of the ices with experimental results for those densities for which data are available.
3. To perform molecular dynamics computer simulations to calculate the thermal conductivity of amorphous ice as a function of the temperature and microscopic porosity of the ice samples.

Progress and results

Computer simulations of bulk amorphous ices at the densities of the two major polymorphs, 0.94 g/cc for low-density amorphous (LDA) ice and 1.17 g/cc for the high-density amorphous (HDA) ice have been performed. The structure of the ices, as determined from the pair-correlation functions, was found to be in good agreement with the correlation functions obtained from neutron scattering experiments. Thus the water models that were used provide a good description of the bulk amorphous ice phases.

Configurations from the bulk simulations were used to generate amorphous substrates. The substrates were equilibrated at 77 K and 10 K for the LDA ice and HDA ice, respectively. After equilibration, water molecules were deposited onto the substrated phase from the vapor phase. The temperatures of the vapor phase molecules were 300 K, to simulate laboratory conditions, and 77 K and 10 K to simulate astrophysical conditions.

Results show that the microporosity of the sample depends upon the temperature of the deposited molecules. The colder the molecules, the more microporous the resulting ice. By depositing water molecules at very low temperatures (10 K) and subsequently heating the resulting microporous ice structure, any desired microporosity can be obtained.

The code has been implemented to calculate thermal conductivity into this molecular dynamics program. It is currently being tested.

Significance of the results

Since all hypotheses about the role of comets in the origin of life and chemical evolution of the solar system make explicit or implicit assumptions about the thermal conductivity of the cometary ice, the results of these calculations will provide crucial information for the critical evaluation of these hypotheses. Recent experiments on laboratory analogs of cometary ice have yielded values of the thermal conductivity that are several orders of magnitude lower than estimates based on other amorphous materials. This has the implication that the interiors of comets are not heated at the perihelion of their orbits.

It is likely that the microporosity of the ice has a significant effect upon the thermal conductivity of the sample. Using computer simulations, the microporosity of the sample can be controlled to a degree that is not possible in the laboratory.

Publications

Jenniskens, P.; Blake, D. F.; Wilson, M. A.; and Pohorille, A.: High Density Amorphous Ice, the Frost on Interstellar Grains. *Astrophys. J.*, 1995, in press.

Keywords

Thermal conductivity, Microporosity, Amorphous ice, Cometary ices

The Use of Nitrous Oxide to Increase Test Times in High-Enthalpy Reflected Shock Tunnels

Investigator(s)

John Cavolowsky and Mark Newfield,
Ames Research Center,
Moffett Field, CA 94035-1000
David W. Bogdanoff, Gregory J. Wilson, and
Myles A. Sussman, Thermosciences Institute,
Ames Research Center

Other personnel involved

Richard J. Exberger, Ames Research Center
William E. Warren, Calspan Corp.,
Ames Research Center

Objectives of the study

The reflected shock tunnel is a common type of ground facility used to produce high-Mach number, high-enthalpy flows. Typical test times for this type of facility are between 1 and 10 milliseconds. Test time increases of 50 to 100 percent would significantly improve the value of reflected shock tunnels. An inexpensive method to increase the test times provided by a given shock tunnel by over 50 percent is to replace the air test gas in the driven tube of a shock tunnel with a mixture of N_2O and N_2 . Such a mixture can be made to have the same elemental composition as air and results in a test gas of the same chemical composition. Preliminary calculations show that the use of N_2O and N_2 allows a given driver to compress a significantly larger mass of driven gas to a specified stagnation enthalpy and, thus, to provide a longer test time.

The main objective of the one-year research effort described herein was to carry out a simultaneous computational and experimental effort to clearly establish whether using nitrous oxide as the driven gas in shock tubes and shock tunnels is an effective way to increase test times. An objective in support of the main goal is to investigate several diagnostic methods for experimentally determining driver gas contamination, which would be useful for flow characterization efforts in any impulse facility.

Progress and results

Numerical simulations provided the basis for the present research. These simulations utilized a one-dimensional code with finite-rate chemistry and a moving mesh. A reaction set appropriate for the N_2O/N_2 mixture was assembled using available liter-

ature. In direct support of the experiments, simulations were performed to specify the precise experimental conditions. One requirement of the experiments was to have equivalent stagnation pressure and enthalpy for both air and nitrous oxide gas mixtures.

A total of 29 shots were made in the electric arc shock tube (EAST) facility. The conditions studied were:

- Reflected shock pressure – 140 atm (18 shots), 70 atm (11 shots)
- Reflected shock region enthalpies – 6.6 to 8.6 MJ/kg
- Driven tube gas – air (18 shots), N_2O/N_2 (10 shots), Ar (1 shot)

The following instrumentation was used (x refers to distance along the facility):

- Static pressures along driven tube (two transducers at different x-positions)
- Static pressures at nozzle exit (two transducers at the same x-position)
- Light emission along driven tube (two photomultiplier tubes (PMTs) at different x-positions)
- Ionization gauge shock detector in driven tube (one gauge)
- Static pressure at nozzle exit (one gauge)
- Total light emission from gas cap of blunt body in center of flow at nozzle exit (1 PMT)
- Light emission at Ar 697 nm line from gas cap of blunt body in center of flow at nozzle exit (monochromator with one PMT)

With this instrumentation, estimates of test time could be made as follows:

1. The time for the slug of test gas to pass a given point in the driven tube could be inferred from the light emission histories along the driven tube.
2. Duration of the test time at the nozzle exit could be inferred from the light emission histories at that location. A fairly abrupt increase in light emission was assumed to signal the arrival of driver gas, both in the driven tube and at the nozzle exit.
3. From the pressure histories at the nozzle entrance the length and quality of the “constant pressure” period could be used to estimate the duration of the test time.

The static pressure data at the nozzle exit proved to be unusable because the violent vibration produced by the reflection of the shock wave from the nozzle

entrance overwhelmed the transducer pressure information that the transducer gathers. Also, there was little difference between the two light histories (total emission, emission at the Ar 697 nm line) obtained from the gas cap over the blunt body at the nozzle exit. It seems likely that the Ar line emission at 697 nm (for the monochromator channel) is overwhelmed by broadband emission. Thus, increases in the output of this PMT data channel do not signal the arrival of driver gas species with any degree of certainty. It clearly is desirable to have a more definitive spectroscopic detection technique for the arrival of driver gas. However, the development of such a technique in the very short facility entry (five weeks) allowed for in the context of a DDF was not possible.

When the facility was operated with undertailored conditions (driver gas lighter than the driven gas) the use of N_2O/N_2 was found to yield little or no increase in test time. When the facility operation was switched to the overtailored mode (driver gas heavier than the driven gas), substantial increases in test time were found to occur when N_2O/N_2 was used. Seven of the later tests in the EAST facility produced a very consistent picture of an increase in test time obtained by substituting N_2O/N_2 for air in the driven tube, as follows:

1. The time of test-gas slug passage inferred from light emission in the driven tube was 100 to 120 μsec with air and 170 to 240 μsec with N_2O/N_2 . (The duration of the test time for either driven tube gas decreases as the enthalpy is increased.)

2. The test time inferred from light emission at the nozzle exit was 430 to 720 μsec with air and 800 to 1080 μsec with N_2O/N_2 .

3. The duration of the constant pressure plateau at the nozzle entrance was typically zero for air and up to 300 μsec with N_2O/N_2 .

4. The ratio of test times (N_2O/N_2 test time/air test time) observed experimentally using the first two techniques listed was previously between 1.55 and 1.95, versus theoretical predictions of 1.60 to 1.65 for the particular enthalpy range of interest.

The authors deemed the data obtained of sufficiently high quality to be published as a preliminary report in the archival literature of the experimental demonstration of the increase in test time achieved by substituting N_2O/N_2 for air in the driven tube of a shock tunnel. The DDF work reported herein should be followed up by definitive research in the EAST facility, likely using a spectroscopic technique to detect the arrival of helium in the driver gas. Such a research effort would allow a definitive publication to be made.

Significance of results

This work provides strong experimental evidence that the use of N_2O/N_2 instead of air in the driven tube of a shock tunnel will increase the length of the slug of the driven gas traveling down the driven tube and will also increase the duration of the test time at the nozzle exit. Reasonable agreement was found between the test time increases observed experimentally and those predicted by theory. These results will give further impetus towards the implementation of the use of N_2O/N_2 to increase test time in a wide variety of shock tube/tunnel facilities using air as the test gas.

Keywords

Nitrous oxide, Shock tunnels, Increase of test time

Ultrasensitive Detection of Atmospheric Free Radical Molecules: A Full-Sensitivity Demonstration Prototype

Investigator(s)

Charles Chackerian,
Ames Research Center,
Moffett Field, CA 94035-1000
Christopher R. Mahon,
Space Physics Research Institute,
Sunnyvale, CA 94087
James R. Podolske,
Ames Research Center

Other personnel involved

Thomas Blake,
Battelle/Pacific Northwest Laboratory,
Richland, WA 99352

Objectives of the study

For the purpose of realizing a full-sensitivity demonstration prototype magnetic-rotation detector of free radical molecules in the Earth's atmosphere, to design and construct a multiple reflection optical cell contained in a solenoid magnetic field axially and radially uniform to ± 5 percent. A total optical path of 25 meters and small cell volume will give (1) parts/trillion detection sensitivity to free radical molecules in the Earth's upper atmosphere; and (2) spatial resolution of about 200 meters in the sky when the magnetic-rotation spectrometer is based on the DC-8 or ER-2 aircraft. This new technique offers advantages over currently

used approaches in terms of much smaller weight and more easily interpretable results.

Progress and results

Iterative computer-aided design (CAD) programs have been written and used (1) to design the solenoid coil configuration so as to give a uniform (± 5 percent) magnetic field in the optical Herriott cell with a field oscillating at 1 KHz; and (2) resistive-inductive-capacitance (RLC) parameters for a resonant solenoid circuit. Nonmagnetic materials were selected for cell construction.

Significance of the results

The design study shows that the desired optical/solenoidal cell and circuitry will weigh on the order of 15 pounds. The power can be supplied with a commercial power supply, which weighs 30 pounds.

Publications

Blake, T. A.; Chackerian, C., Jr.; and Podolske, J. R.:
Prognosis for a Mid-infrared Magnetic Rotation Spectrometer for the in situ Detection of Atmospheric Free Radicals. Paper accepted by J. Applied Optics, 1995.

Keywords

Ultrasensitive detection, Free radicals, Magnetic rotation spectroscopy

Isotopic Analysis of Meteoritic Organosulfur and Organophosphorous Compounds

Investigator(s)

Sherwood Chang, Ames Research Center,
Moffett Field, CA 94035-1000
George Cooper, SETI Institute,
Ames Research Center

Objectives of the study

The hypothesis is that the organic sulfonic and phosphonic acids discovered in the Murchison meteorite are of interstellar origin. To test this hypothesis, the sulfur ($^{36}\text{S}/^{34}\text{S}/^{33}\text{S}/^{32}\text{S}$), carbon ($^{13}\text{C}/^{12}\text{C}$), and hydrogen (D/H) isotope ratios as appropriate for individual (methyl, ethyl, isopropyl, and n-propyl) sulfonic and phosphonic acids extracted from the meteorite were measured. Measured isotopic ratios that are anomalous with respect to bulk meteoritic or other known solar system values are acknowledged to be diagnostic of presolar origins. If the hydrogen bound to carbon is anomalous and the carbon is not, interstellar origins for both may still prevail. Similarly, the observation of a hydrogen or carbon isotope anomaly in the phosphonic acids would indicate that the phosphorous in the same molecule is also guilty-by-association of an interstellar origin.

Progress and results

Measurements of hydrogen, carbon, and sulfur isotopic compositions were made on individual sulfonic acids. Similar measurements of hydrogen and carbon were obtained for phosphonic acids as a group. These analyses are especially interesting since no individual organic compounds have ever been studied for their sulfur isotopic compositions, let alone in combination with their C- and H-isotopic compositions.

For carbon, isotope ratios are reported as parts per thousand deviations from the $^{13}\text{C}/^{12}\text{C}$ ratios in a carbonate standard: $\delta^{13}\text{C} = 1000\{[(^{13}\text{C}/^{12}\text{C}_{\text{sample}})/(^{13}\text{C}/^{12}\text{C}_{\text{standard}})] - 1\}$, with positive values indicating relative enrichment in the heavy isotope. Analogous formulations apply to the isotope ratios of other elements. Our results for carbon in both types of compounds show isotope ratios that deviate from terrestrial values, but remain well within the range of other meteoritic organic compounds. Apparently, the carbon in the sulfonic and phosphonic acids is not anomalous. A monotonic decrease in the $\delta^{13}\text{C}$ values with increasing carbon number in the former compounds, however, suggests the operation of a kinetic isotope effect,

reflecting stepwise synthesis of larger compounds by stepwise reaction from a single-carbon precursor. This conclusion agrees with earlier results obtained with meteoritic carboxylic acids.

Measurements of hydrogen in the sulfonates, however, reveal δD values (relative to standard mean ocean water) ranging from +660 to +700, denoting strong enrichments in deuterium over terrestrial, bulk meteorite, and Giant Planet values. Somewhat lower enrichments are seen in the bulk phosphonic acids. The excess deuterium in the hydrocarbon portions of these compounds reflects strong kinetic isotope effects known to arise from ion molecule reactions occurring under extremely low-temperature conditions consistent with the astrophysical environment of dense molecular clouds. From these results, we infer that the carbon bound to the anomalous hydrogen is also of interstellar origin, although it does not carry a distinctive isotopic signature. This conclusion is consistent with the absence of known reservoirs of sufficient deuterium enrichment in the solar system with which the carbon could have exchanged its original hydrogen atoms.

Stable isotopes of sulfur were measured in methane sulfonic acid extracted from the Murchison meteorite with water. The isotopic composition was found to be $\delta^{33}\text{S} = 2.48$, $\delta^{34}\text{S} = 2.49$, and $\delta^{36}\text{S} = 6.76$ percent (parts per thousand, relative to Canyon Diablo Meteorite standard), indicating small enrichments of these heavy isotopes over ^{32}S . Based upon analysis of more than 60 meteoritic and numerous terrestrial samples, the mass-fractionation lines for sulfur's 3-isotope systems (plots of $^{34}\text{S}/^{32}\text{S}$ vs. $^{33}\text{S}/^{32}\text{S}$ and $^{36}\text{S}/^{32}\text{S}$ vs. $^{34}\text{S}/^{32}\text{S}$) are defined by $^{33}\Delta = \delta^{33}\text{S} - 0.50 \delta^{34}\text{S}$ and $^{36}\Delta = \delta^{36}\text{S} - 1.97 \delta^{34}\text{S}$. From these relations, $^{33}\Delta = 1.24$ percent and $^{36}\Delta = 0.89$ percent, representing anomalous deviations from all known, otherwise mass-dependent, observations. These anomalies, particularly the $^{33}\Delta$, are well outside the range of analytical uncertainty, and are the largest observed in any meteoritic component. Future work will complete analysis of the sulfur isotopic compositions on other alkyl sulfonates.

Significance of the results

Because of its position on the periodic chart (ref. 1), the chemistry of sulfur can produce mass independent isotope fractionations, as does oxygen. From experimental work, others (ref. 2) have observed that, in such

a fractionation process, the magnitude of fractionation for the different isotopically substituted species varies with mass and angular momentum; therefore, anomalies are expected for both ^{33}S and ^{36}S , but not necessarily of the same magnitude. Laboratory experiments (ref. 3) have also confirmed that mass independent fractionations that are mediated by molecular symmetry factors occur. If the source of fractionation is chemical, this means that the sulfur isotopic anomaly was established in the gas phase, possibly from reactions involving symmetric CS_2 as a precursor to sulfonic acids. The deuterium isotope anomaly in the same molecules suggests that the sulfur isotopic anomaly was also produced by interstellar chemistry. The discovery of an anomalous sulfur isotopic composition in a specific molecule containing excess deuterium is an important advance in the understanding of the cosmochemistry of sulfur.

Meteorites are believed to have been among the building blocks of planets. The observation of isotopic anomalies in sulfur and phosphorous-bearing compounds in the Murchison meteorite would demonstrate for the first time that S and P, along with other of the biogenic elements (H, C, N, O, S, and P) used by life can be traced directly back to the interstellar cloud of gas and dust that spawned the solar system. If early

on these compounds survived delivery to Earth, they may have contributed to the inventory of organic matter available for the origin of life.

Publications resulting from study

Cooper, G. W.; and Chang, S.: Isotopic Measurements of Organic Sulfonates from the Murchison Meteorite. *Lunar and Planet. Science*, vol. XXVI, 1995, pp. 281–282.

References

1. Thiemens, M. H.; and Jackson, T.: *Lunar and Planet. Science*, vol. XXVI, 1995, pp. 1405–1406.
2. Mauersberger, K.; Morton, J.; Schveler, B.; Stehr, J.; and Anderson, S. M.: Multi-isotope Study of Ozone—Implications for the Heavy Ozone Anomaly. *Geophys. Res. Letters*, vol. 20, no. 11, June 7, 1993, pp. 1031–1034.
3. Bains-Sahota, Swroop, K.; and Thiemens, Mark H.: A Mass-independent Sulfur Isotope Effect in the Nonthermal Formation. *J. Chem. Phys.*, vol. 90, June 1, 1989, pp. 6099–6109.

Keywords

Meteorites, Organic compounds, Stable isotopes

Development of Fiber-Optic Sensors for Studies of Transition from Laminar to Turbulent Flow

Investigator(s)

Y. C. Cho, N. N. Mansour,
and R. D. Mehta, Ames Research Center,
Moffett Field, CA 94035-1000

The goal of this study is to develop a novel transducer technique for real-time measurements of pressure fluctuations in conjunction with studies of the transition from laminar flow to turbulence on an airfoil surface. One of the major tasks in information science is collecting information (sensing or measuring). Measurements in physical sciences are accomplished through interaction of sensors with the system involving the measurand. The interaction should be large enough for a good signal-to-noise ratio, and yet should not be so large as to cause excessive disturbance to the system. Aerodynamic systems involving transitions are often extremely sensitive to a transducer intrusion, which is difficult to avoid with existing sensor techniques. The proposed program will exploit fiber-optic (FO) sensor technology, which has been maturing in

various industrial applications as well as in research. This technology offers many advantages for aerodynamic studies, including high sensitivity, a compact sensor package, a wide dynamic range, a high frequency response, and geometric versatility. The high sensitivity and the compact size can be utilized to minimize flow/sensor interaction noise. The geometric versatility provides great flexibility in configuring the optical fiber as extended sensor elements or sensor arrays. The optical fibers can be implanted on the surface of a solid body, or they can be flush mounted on a surface such as an airfoil with perforation for laminar flow control. Such sensor implanting or mounting is a desirable feature for minimizing flow/sensor interaction noise. Some other advantages of FO sensors include superb telemetry capability, high temperature tolerance, and immunity to electromagnetic interferences. These features are also important in aircraft design as well as in the wind-tunnel test environment.

Keywords

Fiber-optic sensor, Flow transition studies

Size-Density Studies of Chondrules, and Aerodynamic Sorting in the Solar Nebula

Investigator(s)

Jeff Cuzzi, Ames Research Center,
Moffett Field, CA 94035-1000
Julie Paque, SETI Institute,
Ames Research Center

Other personnel involved

Monica Rivera, Summer High School
Apprenticeship Program

Objectives of the study

Chondrules are millimeter-diameter, solidified drops of liquid silicate rock. They are the dominant constituent of the very primitive "chondritic" meteorites, and they show clear evidence for aerodynamic sorting. The properties of chondritic meteorites, or chondrites, are unexplained and have puzzled meteoriticists for over a century. The objective of this study is to examine the relationship between size, density, texture, and rim characteristics of chondrules in several different chondrite types (unequilibrated ordinary, carbonaceous, and enstatite chondrites) and determine what characteristics are a reflection of conditions during formation and residence in the nebula. This information will be used to test and constrain plausible models for the origin and early evolution of primitive meteorite parent bodies in terms of specific nebular processes. Whether the distribution of chondrules in various classes of chondrites can be explained by aerodynamic sorting in the nebula will be examined, and the extent to which the inclusion of the rim with the chondrule improves or degrades the agreement with an aerodynamic sorting hypothesis will be studied.

Progress and results

In order to examine the relationship between size, density, texture, and composition of chondrules from a meteorite, it is necessary to separate, or disaggregate, the sample. A 5-gram sample of the Allende carbonaceous chondrite has been successfully disaggregated by repeated cycles of freezing and thawing of the sample. A total of 287 round objects were identified, weighed, measured, and mounted for petrographic and chemical examination. Not all of these 287 objects are chondrules, and those that are not will be eliminated from the data set after petrographic examination. Petrographic and chemical examination of the Allende samples are currently under way. Disaggregation of two additional meteorites, both of slightly higher metamorphic grade than the Allende sample, has not been as successful. The experimental procedure is currently being evaluated, and modifications will be made in an effort to enhance the disaggregation process. The availability of lower metamorphic grade samples, which will be easier to disaggregate (and probably more characteristic of direct nebula aggregates), is being explored.

Significance of the results

This project has been under way for only two months. Further examination of the data must be performed before the results can be evaluated in the context of conditions in the solar nebula.

Keywords

Meteorites, Solar nebula, Aerodynamic sorting

Effects of Stratospheric Ozone Depletion and Increased Levels of Ultraviolet Radiation on Plants of Arizona

Investigator(s)

Hector L. D'Antoni,
Ames Research Center,
Moffett Field, CA 94035-1000
Joseph W. Skiles,
Johnson Controls World Services,
Ames Research Center

Other personnel involved

Jeraldine Mazzurco, Dan Levy, and
Heather Brady, Ames Research Center

Objectives of the study

To identify and measure indicators of the effects of increased solar ultraviolet (UV)-B radiation on terrestrial plants in order to acquire a capability to predict the consequences of further increased UV-B radiation on terrestrial ecosystems.

Progress and results

Research was initiated at the Ames Research Center. A small shed was built and screening material tested to create a moderate UV-B screening ambient and a UV-B exclusion ambient. Several experiments were performed in order to calibrate the techniques. They allowed adjustment of the chlorophyll extraction technique, and calibration of a nondestructive chloro-

phyll measuring device in terms of mg of chlorophyll per sample. Differences in growth were estimated by measuring internodal distances in plants grown under each treatment. Aging of screens was monitored with an OL-752-O-PMT spectroradiometer. Measurements of solar irradiance for the 250–800 nm range were performed at a spectral resolution of 2 nm.

Publications

None yet. D'Antoni's presentation of remote sensing and past global changes at the University of Puerto Rico, Mayagüez Campus (UPRM) was the first technical seminar of the NASA-sponsored Tropical Center for Space and Earth Studies. About 75 high school science teachers toured the field facility last summer as part of the program of the Global Change Science Institute sponsored by the University of California, Berkeley, and the National Science Foundation (NSF). The tours enabled the teachers to observe field experimentation in UV-plant response. Skiles presented a seminar to each of the groups on ozone depletion and the consequences for the biosphere.

Keywords

Ozone depletion/UV-B radiation, Plant responses to increased UV-B radiation

Return to the Red Planet: Remote Sensing Analog Studies as Preparation for Mars Exploration Exobiology

Investigator(s)

Jack D. Farmer and James Brass,
Ames Research Center,
Moffett Field, CA 94035-1000

Objectives of the study

In 1976, the U.S. sent two landers to the surface of Mars to search for evidence of life. Martian soils sampled by both Viking mission landers are devoid of organic materials. While the present surface environment of Mars appears to be inhospitable to life as we know it, interestingly, the Viking orbital missions provided a contrasting view of the earlier history of Mars. The presence of water-carved channels and paleolake basins in orbital images indicate that Mars was much more Earth-like earlier in its history, with a denser, warmer atmosphere and abundant surface water. Not surprisingly, in recent years, the exploration for Martian life has shifted focus from extant life to the search for evidence of an ancient biosphere. It is plausible that life developed on Mars earlier in its history and then died out in surface environments as the planet lost its atmosphere and began to refrigerate. Although there is a chance that life may yet survive in the subsurface where liquid water is stable, access to such environments will require deep drilling and technologies that are presently beyond the scope of planned robotic platforms. It is likely that, if life did develop on Mars during an earlier clement period, it left behind a fossil record either as actual permineralized organic remains of microorganisms, or their biochemical signatures. Studies of ancient rocks on Earth indicate that the most favorable environments for the long-term preservation of microorganisms are those in which minerals precipitate from solution, entrapping living organisms. The search for extant life on Mars has often been equated to the search for liquid water. In parallel fashion, the exploration for extinct life (a fossil record) may be equated to the exploration for key aqueous mineral deposits. Central to a strategy to explore for a fossil record on Mars is to locate aqueous mineral deposits that formed under such conditions, but Mars is a large planet with a complex surface and history. How do we go about systematically exploring for a fossil record there within the tight technological and budgetary constraints of future missions? This study is aimed at the detection of such deposits from Mars orbit. The primary goal is to define the basic

spectral and spatial resolution requirements needed to identify high-priority targets for future landed missions for Mars exopaleontology. This activity is regarded as a fundamental step toward Mars sample return, presently slated for the year 2005. Instrumentation for pinpointing the surface locations of aqueous mineral deposits from orbit are presently poorly constrained.

Progress and results

In 1995 the initial study utilized hyperspectral, high spatial resolution near-infrared (NIR) images of the Mono Basin (a primary Mars analog site in eastern California) to simulate the lower resolution instruments being flown during upcoming orbital missions. Goals included determining the threshold resolution requirements and data analysis methods needed to identify discrete mineralogies from Mars orbit. By combining the information of adjacent pixels in high-resolution data sets, the resolutions that will be obtained from the Mars missions in 1996 and 1998 can be simulated. Realistic thresholds for spatial and spectral resolution needed to recognize discrete mineral deposits from Mars orbit can also be identified. This information will be used to define nominal instrumentation requirements for future orbital missions that will provide a foundation for future landed missions for exopaleontology.

The study began with visible NIR imaging of the Mono Basin, which was used to plan field strategies and develop preliminary image-based geological maps. High-resolution NIR scenes of the Mono Basin were then obtained from the Advanced Visible and Infrared Imaging Spectrometer (AVIRIS), and the pure "end-member" pixels were identified within each scene. The spectra of these end-member pixels were extracted and compared to published spectral libraries. Initial efforts focused on exploring carbonate and evaporite deposits in the Mono Basin, primary mineral targets for Mars exopaleontology. Field-based geological mapping of the Mono Basin was accomplished in order to ground-truth pixel compositions. Field observations revealed the compositions of the end-member pixels identified in the images to be mixed, containing obvious spectral contributions from a number of different minerals and vegetation types. The full range of rock and mineral types within end-member pixels were sampled for acquisition of lab spectra. Thus a library of more reliable composite

spectra, which will aid in digital mapping and identifying threshold resolution requirements, can be built. Preliminary spectral comparisons established the need for a more sophisticated pure end-member analysis, one that will integrate both field and lab-based observations to create a more reliable spectral library for mapping purposes. To accomplish this goal in 1996, a cutting edge software package (ENVI), which utilizes multivariate statistical approaches to identify pure

end-members from hyperspectral imaging data (such as AVIRIS), has been acquired. Among the other major objectives for 1996, the spectral library of individual minerals and composite spectra specific to the Mono Basin will be expanded, and other high-priority targets, such as thermal spring deposits, will be added.

Keywords

Mars, Martian life, Mono Basin

Laser-Spectroscopic Instrument for Turbulence Measurements

Investigator(s)

Douglas G. Fletcher,
Ames Research Center,
Moffett Field, CA 94035-1000

Objectives of the study

To develop and demonstrate a laser-spectroscopic instrument that can be used to obtain simultaneous measurements of temperature, density, pressure, and velocity in unseeded, turbulent, compressible air flows.

Progress and results

A new velocity measurement technique using flow-tagging of atomic oxygen is being developed for incorporation into a demonstrated capability for measuring thermodynamic properties using laser-induced fluorescence of O_2 . It is envisioned that the interdependence of thermodynamic and velocity fluctuations caused by turbulence could be directly investigated through applications of this previously unavailable instrumental capability. For example, this nonintrusive instrument would allow a direct assessment of the assumption that all of the aforementioned fluctuating quantities are uncorrelated, and therefore do not have to be included in numerical models.

The viability of atomic oxygen is being established as a useful flow-tag species. Using existing laser instrumentation, populations of atomic oxygen were created in room air and probed at successively greater time delays to evaluate photochemical mechanisms

that would deplete the tag population and limit the applicability of the approach. In addition, through collaboration with other researchers, the feasibility of using ozone as a flow-tag species for extremely long time delays was investigated. A thorough understanding of the 193-nm induced photochemistry has been developed.

The next phase of this investigation will be directed towards the demonstration of the velocity measurement approach in a small-scale, free-jet air-flow facility. This will involve upgrading the camera system to an intensified charged coupled device (CCD) system to increase the detected signal-to-noise ratio. In addition, the integration of the velocity measurement approach into the existing thermodynamic property measurement capability will continue.

Publications resulting from study

1. Fletcher, D. G.: Two-Photon Excitation of Atomic Oxygen Using a Raman-Shifted, ArF-Excimer Laser. *Applied Physics B*, vol. 60, 1995, pp. 61-65.
2. DeBarber, P. A.; Segall, J.; Brown, M. S.; Pitz, R. W.; Brown, T. M., III; and Fletcher, D. G.: Ozone Flow-Tagging: a Novel Approach for Unseeded Velocity Measurement. AIAA Paper 95-1952, presented at the AIAA 26th Plasmadynamics and Lasers Conference, San Diego, Calif., June 1995.

Keywords

Lasers, Velocimetry, Fluorescence

Biotechnical Applications of Reusable Surface Insulation

Investigator(s)

Howard E. Goldstein and Daniel B. Leiser,
Ames Research Center,
Moffett Field, CA 94035-1000

Objectives of the study

To modify the characteristics of the reusable surface insulation (RSI) used on the Space Shuttle to improve its potential usability as a bone implant. Every year trauma, disease, surgery, and degenerative aging processes require hundreds of thousands of orthopedic and dental procedures that in turn require bone implants. The goal of this research is to modify RSI to fill the need for a bone implant material that preserves active function and eliminates the toxicities associated with currently used hardware (i.e., metals), yet is biocompatible and resistant to wear, corrosion, breakage, and loosening.

Progress and results

The tile morphology was modified to increase the pore size by a variety of methods. The most effective was to add a sacrificial fiber to the original slurry that burned out during sintering. Results from animal implant studies have shown that the biocompatibility of modified RSI is very good and that no signs of rejection by

the body are evident. The improved pore structure has allowed bone ingrowth to the extent that it appears that a viable living composite has formed. Current work is attempting to optimize the RSI pore structure and strength. The composition and processing of the RSI materials are being modified to obtain more uniform materials that have higher strength and an optimum distribution of pore sizes. Samples that have been implanted and retrieved from the experimental animals will be tested for mechanical properties. A new series of implant tests will be performed to verify and extend the data obtained so far. Once an optimum material has been developed, the processing technology will be transferred to Biomedical Enterprises for commercialization.

Significance of the results

The ultimate result of this research project might be to produce implants that are as viable as the natural bone. The payoff in terms of ameliorating human suffering is potentially enormous.

Keywords

Bone implant, Reusable surface insulation, Biocompatibility

Computational Modeling of Ultrafast Optical Pulse Propagation in Semiconductor Lasers and Amplifiers

Investigator(s)

Peter M. Goorjian,
Ames Research Center,
Moffett Field, CA 94035-1000
Govind P. Agrawal,
The Institute of Optics,
University of Rochester,
Rochester, NY 14627

Other personnel involved

Andrew Hulse, Andre Knoesen, and
John Heritage, University of California, Davis,
Davis, CA 95616

Objectives of the study

To understand the emerging technology of photonic (or optoelectronic) integrated circuits (PICs or OEICs). In PICs, optical and electronic components are grown together on the same chip. To build such devices and subsystems, one needs to model the entire chip. The importance of PICs is in their use in building integrated optical transmitters, integrated optical receivers, optical data storage systems, optical interconnects, and optical computers.

This research will provide accurate computer modeling of electromagnetic wave propagation in semiconductors. Such modeling is necessary for the successful development of PICs. More specifically, these computer codes will enable the modeling of such devices, including their subsystems, such as semiconductor lasers and semiconductor amplifiers in which there is femtosecond pulse propagation. One test simulation will be the amplification of a femtosecond optical pulse in a semiconductor. The computed results will be compared to experimental results.

Progress and results

The theory and governing equations have been formulated for modeling the propagation of 50–100-femtosecond pulses in semiconductor amplifiers. A finite-difference algorithm has been developed that solves the nonlinear Maxwell's equations and the semiconductor Bloch's equations. These combined equations will model the optical

pulse and the interband and intraband dynamic processes in the semiconductor. Presently, this algorithm is being implemented into a code that has been used to simulate light bullets.

The capability of the algorithm in nonlinear glass-like materials has been demonstrated by calculations of light bullets (ref. 1), i.e., optical pulses that are self-supporting under the effects of diffraction, anomalous dispersion, and nonlinear refraction. These pulses propagate stably, without any essential changes in shape or spectral content.

Figure 1 shows two counter-propagating light bullets, which change each other's trajectories during their interaction.

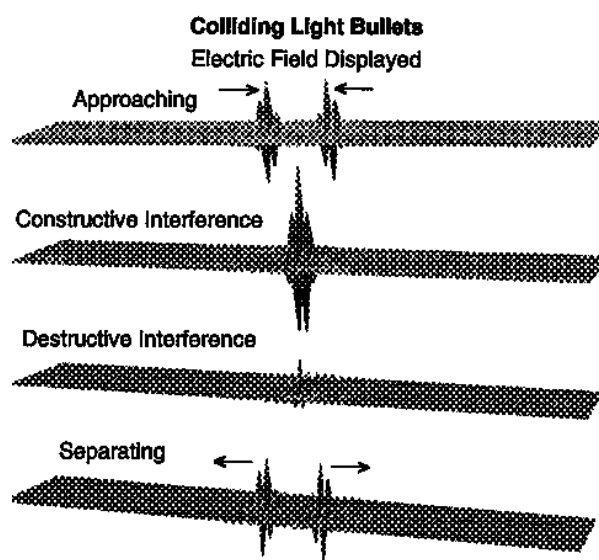


Figure 1. The electric field of two counter-propagating light-bullet-like pulses after 155 fs, 310 fs, 465 fs, and 620 fs of propagation.

Significance of the results

These calculations of propagating and scattering light bullets show that this algorithm has the capability of modeling electromagnetic fields in nonlinear optical materials.

References

1. Goorjian, P. M.; and Silberberg, Y.: Numerical Simulations of Light Bullets, Using the Full Vector, Time Dependent, Nonlinear Maxwell Equations. Integrated Photonics Research Topical Meeting (IPR'95), Dana Point, Calif., Feb. 23–25, 1995.

Keywords

Computational nonlinear optics, Semiconductor lasers and amplifiers, Ultrafast (femtosecond) optical pulse propagation

A Long-Duration Test Flight of a Superpressure Balloon as a Platform for Mars Exploration

Investigator(s)

Robert M. Haberle, G. Scott Hubbard,
Lawrence G. Lemke, and Geoffrey A. Briggs,
Ames Research Center,
Moffett Field, CA 94035-1000

Other personnel involved

James Cantrell, Utah State University,
Logan, UT 84322-4140

Objectives of the study

To demonstrate that a superpressure balloon made from Biaxial Nylon 6 can survive for at least one year in the Earth's stratosphere at 120,000 feet, where the pressure and temperature conditions are similar to those expected on Mars.

Progress and results

A single balloon was launched during the first year; the launch was only partially successful because of a premature firing of the cutdown system at lift-off. For the second year of the project, the payload mass was reduced in order to avoid the Federal Aviation Administration's (FAA's) requirement of flying a cutdown system for payloads weighing more than 8 kg. The resized payload was tested and readied for launch, but it has not been launched yet because of numerous delays.

Significance of the results

Because no launch has occurred, there are no results to report. The launch is planned for early 1996.

Keywords

Mars, Superpressure balloon, Biaxial Nylon 6

Remote Sensing of Aircraft Contrails Using a Field Portable Imaging Interferometer

Investigator(s)

Philip D. Hammer,
Ames Research Center,
Moffett Field, CA 94035-1000
William H. Smith,
Washington University,
St. Louis, MO 63130

Other personnel involved

Stephen Dunagan and Anthony Strawa,
Ames Research Center

Objectives of the study

To measure visible and infrared radiative effects of aircraft contrails to provide information about their spatial distributions, their microphysical properties (especially ice crystals), their time evolution, and their surroundings by application of a novel remote sensing technique, imaging interferometry. The instrument concept to be utilized is called DASI (digital array scanned interferometry). These measurements will be made from the ground at appropriately selected sites. Analytical techniques employing atmospheric radiative transfer methods will be developed and applied to analysis and interpretation of the spectral images. The overall objective is to demonstrate the feasibility of this measurement technique for remote sensing of contrail properties, and more generally, of aerosol plumes.

Progress and results

Preparation is under way for participation in a coordinated field experiment at a site in Oklahoma during

Apr. 1996. Ground-based measurements of aircraft contrails and cirrus clouds together will be made with other participating sensors. Airborne and satellite-based measurements by collaborating investigators are also planned. This experiment will be an opportunity to apply our contrail measurement technique and coordinate our results with the other experimenters, which is an ideal situation for carrying out case studies as well as validation of our technique.

Concurrently, analysis algorithms are being developed for the interpretation of the data acquired at the Oklahoma site as well as at other ground-based locations.

To date, progress has been made in the configuration of the sensors. The near-infrared sensor is operational and has recently been deployed on the NASA C130 aircraft for land observations. Development is under way on the visible sensor.

Significance of the results

The preliminary results from the aircraft measurements have provided diagnostic and engineering information that will be essential for the contrail measurement preparations.

Keywords

Aircraft contrails, Remote sensing, Imaging spectrometers

Development of Noninvasive, Tissue-Oxygen Sensor for Optimizing Ergonomic Design of Workstations in Space and on Earth

Investigator(s)

Alan R. Hargens, Ames Research Center,
Moffett Field, CA 94035-1000
Gita Murthy, University of California, San Diego,
Ames Research Center
Norman J. Kahan, Pacific Sports Physicians,
Cupertino, CA 95014
David M. Rempel, University of California, San
Francisco, San Francisco, CA 94143
Yvonne A. Clearwater, Ames Research Center
Bruce W. Webbon, Ames Research Center

Objectives of the study

Repetitive motion disorders of the hand and forearm are caused by repeated exertion of a specific muscle, tendon, or joint. Such repeated activities, over time, may increase local tissue fluid pressure, decrease local blood flow and tissue oxygenation, and cause pain and functional deficits of the involved limb (refs. 1 and 2). Examples of repetitive motion disorder are carpal tunnel syndrome (CTS) and epicondylitis. In Santa Clara County, California, alone, over 7000 cases of CTS were reported in 1988 (ref. 3). At present there is no noninvasive method to monitor local tissue stress and its impact on tissue oxygenation. Such a technique will help improve designs of keyboards, gloveboxes, and other workstations for prevention of CTS.

A current procedure for studying CTS and monitoring local tissue stress is to measure tissue fluid pressure by catheter insertion (refs. 4–6). Because of the invasive nature of this technique, application of this procedure to evaluate risk factors for jobs and tasks is difficult. If tissue oxygenation can be accurately measured noninvasively, it may be a valuable tool for identifying tasks/tools with high risk for repetitive motion disorders. Dual-wave near infrared (NIR) spectrophotometry is a noninvasive technique that exploits the disparity between absorption spectra of oxy- and deoxyhemoglobin to measure changes in tissue oxygenation (fig. 1). A disadvantage of the NIR technique is that currently available probes are designed for deep penetration of skeletal muscle and consequently are inappropriate for monitoring small, more superficial tissues. Therefore, the objective of this study is to develop a probe such that superficial tissue

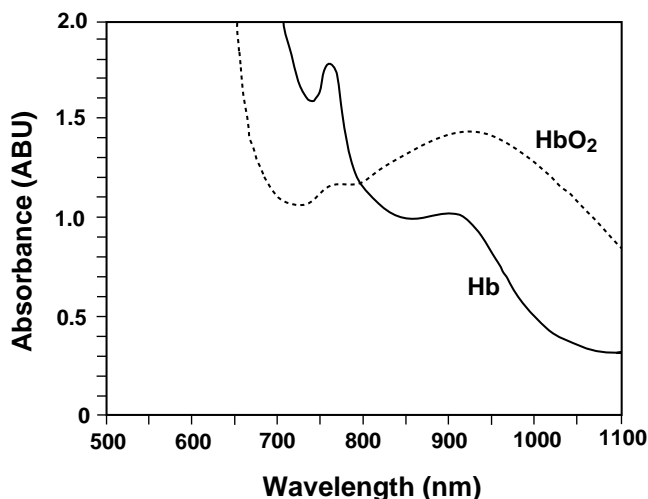


Figure 1. The absorption spectra for oxyhemoglobin (HbO₂; dashed line) and deoxyhemoglobin (Hb; solid line). The instrument measures reflected light at 760 and 850 nm. Deoxyhemoglobin and deoxymyoglobin absorb more light at 760 nm, whereas oxyhemoglobin and oxymyoglobin absorb more light at 850 nm.

can be studied. As a first step, tissue oxygenation in the superficial extensor carpi radialis brevis muscle of the forearm is investigated during rest and different levels of isometric contraction.

Progress and results

The NIR probe consists of a light source and a detector (fig. 2). The light sources (tungsten filament lamps) emit light into tissue. Light is scattered randomly within the tissue; some of it is absorbed by the tissue and some reflects back to the photodetectors located on the probe. The probe, which illuminates the sample tissue, is designed to penetrate to depths of 2–3 cm. However, the extensor carpi radialis muscle belly lies only 1–2 cm beneath the skin (seen by ultrasound imaging). One way to reduce the photon penetration depth is to decrease the light source to detector distance. The probe was redesigned so that the distance between the light source and the detector can be adjusted to allow light penetration 0.85–2 cm below the skin. Using the modified adjustable probe, tissue oxygenation was measured in 3 subjects in the

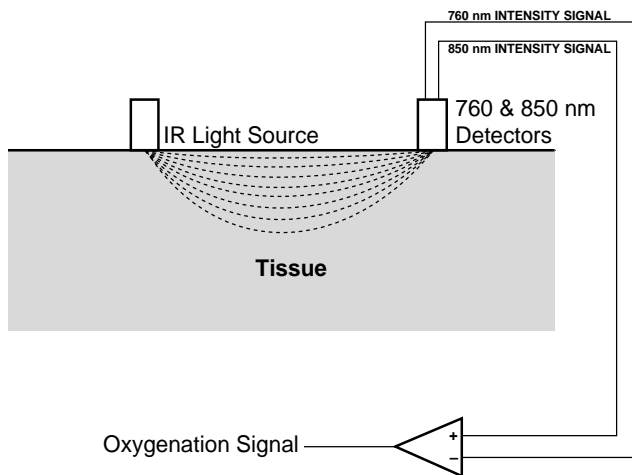


Figure 2. Principle of operation of the dual-wave NIR spectrophotometer. IR energy emitted by the light source is scattered randomly within the tissue and sensed by two photodetectors, equipped with optical bandpass filters of 760 and 850 nm wavelengths, respectively. Optical densities of blood hemoglobin at 760 and 850 nm are dependent on oxygenation state. The two intensity signals are passed through a differential amplifier, the output of which is an index of tissue oxygenation that is relatively invariant with changes in overall hemoglobin concentration. Depth of light penetration is a function of separation between the light source and the detectors. The distance between light source and detectors in this study allowed measurements at an average depth of 2.5 cm below the skin.

extensor carpi radialis muscle of the forearm during 15 seconds of baseline, 100, 5, 10, 15, 20, 40, 80, and 100 percent maximum voluntary contraction (MVC). Each level of percent MVC was separated by 30 seconds of recovery. Preliminary data indicate that tissue oxygenation decreases linearly from 5 percent MVC to 40 percent MVC (fig. 3). In most subjects, tissue oxygenation increased by 15 and 20 percent above baseline during 5 percent MVC, probably because of increased muscle blood flow during exercise.

Significance of the results

The adjustable probe enables the study of superficial tissue such as the extensor carpi radialis. Potentially, this technique can be extended to study the carpal tunnel of the wrist. CTS is the most common work-related compression neuropathy in humans. In CTS, the symptoms occur because a major nerve is compressed by tendons and edema fluid as it passes through a narrow channel of bone and ligament at the wrist. Edema in the carpal tunnel may cause oxygen

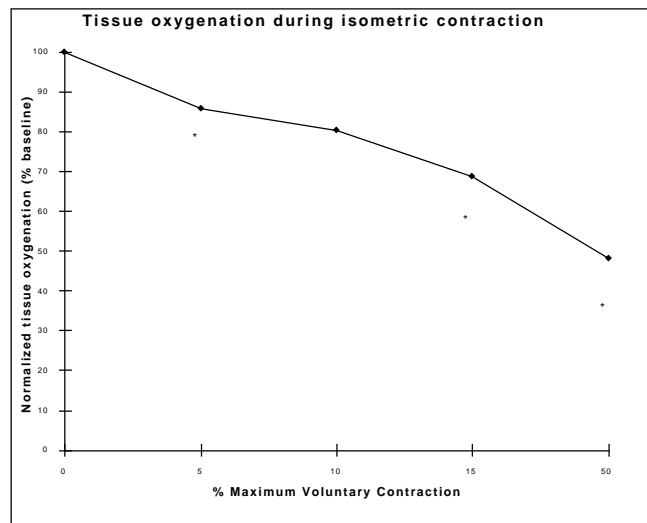


Figure 3. Tissue oxygenation as a function of level of isometric contraction of a forearm muscle.

depletion, which may, in turn, detrimentally affect wrist function. The incidence of CTS is greatly increasing with increased use of computer keyboards and automated machinery. CTS is becoming common to many occupations involving repetitive hand motions, including computer terminal operators, typists, electronic assembly workers, butchers, musicians, garment workers, grocery checkers, carpenters, and packers. Moreover, in most of these occupations, repetitive force exertions are major risk factors in causing such cumulative trauma. Typists and computer operators, for example, exert no more than 1–5 percent MVC. However, when such a small magnitude of force is exerted over a prolonged period of time, tissue edema and deoxygenation may occur.

Astronauts will work for prolonged periods of time at computer keyboards during tours of duty aboard Space Station, as well as on interplanetary missions. Because of physiological changes in the hand experienced in microgravity, including a lowering of blood pressure and local swelling, astronauts working at keyboards are predicted to be at increased risk of developing symptoms of CTS during prolonged spaceflight. In addition, problems with hands have begun to be identified in extravehicular activity (EVA)-related tasks. Recent evidence indicates that some astronauts have difficulty donning their EVA gloves because of hand swelling and subsequently, they experience coldness in their hands while working in their space suits (Webbon, personal communication). Both swelling and coldness (decreased blood flow) are important factors that predispose crew members in space to hand fatigue and CTS.

Therefore, via the approach described in the present report, the investigators intend to improve work environments on Earth and in space through the development of a noninvasive device for monitoring and understanding work-related repetitive motion disorders.

Publications resulting from study

Hargens, A. R.; Ballard, R. E.; Wilson, M.; Torikoshi, S.; Murthy, G.; Breit, G. A.; Watenpaugh, D. E.; Kawai, Y.; and Yost, W. T.: Noninvasive Intracranial Pressure and Tissue Oxygen Measurements for Space and Earth. Presented at Life Sciences and Space Medicine Conference, Houston, Tex., Apr. 3-5, 1995, pp. 130-131.

Murthy, G.; and Hargens, A. R.: Near Infrared Spectroscopy: A Noninvasive Technique for Diagnosing Exertional Compartment Syndrome. *Operative Techniques in Sports Medicine*, vol. 3, no. 4, 1995, in press.

References

1. Hargens, A. R.: *Tissue Nutrition and Viability*. Springer-Verlag, New York, 1986.
2. Rempel, D. M.; Harrison, R. J.; and Barnhardt, S.: Work-related Cumulative Trauma Disorders of the Upper Extremity. *J. Am. Medical Assoc.*, vol. 267, 1992, pp. 838-842.

3. Occupational Disease Surveillance: Carpal Tunnel Syndrome. *Morbidity and Mortality Weekly Report*, vol. 38, 1989, pp. 485-489.
4. Gelberman, R. H.; Hergenroeder, P. T.; Hargens, A. R.; Lundborg, G. N.; and Akeson, W. H.: The Carpal Tunnel Syndrome: A Study of Carpal Canal Pressures. *J. Bone and Joint Surgery*, vol. 63, 1981, pp. 380-383.
5. Hargens, A. R.: Measurement of Tissue Fluid Pressure as Related to Nerve Compression Syndromes. In *Nerve Compression Syndromes*, R. M. Szabo, ed., SLACK, Thorofare, N. J., 1989, pp. 41-65.
6. Hargens, A. R.; Akeson, W. H.; Mubarak, S. J.; Owen, C. A.; Gershuni, D. H.; Garfin, S. R.; Lieber, R. L.; Danzig, L. A.; Botte, M. J.; and Gelberman, R. H.: Tissue Fluid Pressures: From Basic Research Tools to Clinical Applications (Kappa Delta Award Paper). *J. Orthopaedic Res.*, vol. 7, 1989, pp. 902-909.

Keywords

Tissue oxygenation, Near-infrared spectrophotometry, Repetitive trauma disorders

A Novel Telemetric Biosensor to Monitor Blood pH Online

Investigator(s)

John W. Hines, Ames Research Center,
Moffett Field, CA 94035-1000
Sara B. Arnaud, Ames Research Center

Other personnel involved

Chris Soms, Ames Research Center
Marc Madou, Microfabrication Applications,
Palo Alto, CA 94306
Lynn Kim, Ames Research Center
Jennifer Garrison, Foothill-De Anza
Community College District Programs,
Ames Research Center
Michael Harrison, University of California,
San Francisco, Fetal Treatment Center,
San Francisco, CA 94143

Objectives of the study

No known wireless telemetric devices that allow chronic, in vivo measurements of pH presently exist. NASA needs such devices to better understand physiological changes induced by the space environment. The medical community needs this capability as a monitoring and diagnostic tool with ambulatory and fetal patients. The objectives of this study are threefold: 1) to design, fabricate, and test a catheter-based microsensors for chronic, online monitoring of blood and tissue pH levels; 2) to modify an existing, totally implantable biotelemeter to acquire, process, and transmit the pH signals; and 3) to perform in vivo testing of the pH sensor and biotelemeter.

Progress and results

pH Probe

A miniaturized pH probe based on a solvent, polymeric H⁺-sensitive neutral carrier membrane cast around the tip of a microbore catheter has been designed, fabricated, and tested. It consists of two single lumen catheters (physically combined or separated); one lumen each for the reference and pH electrodes. The miniaturized sensors exhibit response characteristics similar to larger, commercially available pH electrodes. Baseline drift is linear, predictable, and on the order of 1–2 mV (0.01–0.03 pH units) every 24 hours. Sensor sensitivity is in the theoretical range

of 57–60 mV/pH unit at room temperatures. Sensitivities are very stable, drifting less than 1 percent over a 7-day period. Response times are rapid, with approximately 95 percent of the response achieved within less than 3 seconds.

Electrodes have been implanted intravascularly in sheep for a few hours, and subcutaneously in rodents for periods up to 5 days. Some electrodes have performed well in vivo, exhibiting baseline and sensitivity drift similar to that found on the bench. Other electrodes, more commonly reference electrodes, “fail” after just a few days of implantation. Failures appear to be mechanical in nature, e.g., fluid leakage into interconnects, damage to membrane due to animal movement, etc. Extensive effort is now under way to improve electrode physical durability.

Biotelemetry

A totally implantable, digitally encoded biotelemeter for measurement of pH, temperature, and heart rate has been designed, prototyped, and successfully bench tested in conjunction with the microbore pH electrode. The circuit employs a low-power analog-to-digital (A/D) converter, a digital-encoding integrated circuit (IC) (Manchester), and transmits a pulse-modulated 455-kHz carrier. It dissipates less than 120 μ A. The device has been miniaturized in thick film hybrid form and will be packaged with a 3/4-ampere-hour battery inside a biocompatible ceramic enclosure. A portable receiver acquires and demodulates the radio frequency (RF) carrier, demultiplexes and decodes the 4 data channels, and presents the output to liquid crystal displays (LCDs) on the front of the receiver chassis. A prototype receiver has been successfully tested with implants in sheep.

Significance of the results

A novel biotelemetry system that integrates a miniaturized, neutral carrier-based pH probe, a totally implantable, digital biotelemeter, and a portable, easy-to-use receiver has been designed, fabricated, and tested. Initial application of this technology will be to improve human fetal monitoring at the University of California, San Francisco's Fetal Treatment Center. Ultimately, the technology will be used with animal models on the Space Station to further understand physiological adaptation to the space environment.

Publications

Hines, J. W.; Somps, C. J.; Ricks, B.; and Kim, L.:
Advanced Biotelemetry Systems for Space Life
Sciences: pH Telemetry. In proceedings of the 13th
International Symposium on Biotelemetry,
Williamsburg, Va., Mar. 26-31, 1995.

Hines, J. W.: Medical and Surgical Applications of
Space Biosensor Technology. In proceedings of the
46th International Astronautics Congress, Oslo,
Norway, Oct. 2-6, 1995.

Keywords

pH sensor, Biotelemetry, Fetus

Global Climate Change: The Role of Electron-CO₂ Collisions in the Cooling of the Thermosphere

Investigator(s)

Winifred M. Huo,
Ames Research Center,
Moffett Field, CA 94035-1000

Objectives of the study

To determine quantitatively how electron-CO₂ collisions affect the cooling of the thermosphere.

Progress and results

CO₂ is a major greenhouse gas whose concentration has been steadily increasing. It absorbs radiation at 15 micron wavelength, exciting its ν_2 bending mode. In the troposphere, the vibrational excited CO₂ is quenched by collision with other atoms or molecules and the radiation energy absorbed by CO₂ is converted into kinetic energy, resulting in global warming. In the stratosphere and above, the fine-structure changing collisions of the oxygen atom with CO₂ will also excite the latter to the ν_2 mode. Because of the significantly lower density in the upper atmosphere, radiation instead of collisional quenching is the major dissipation mechanism, and it results in thermospheric cooling. These considerations indicate that increased CO₂ concentration has opposite effects in the troposphere and thermosphere. Thermospheric cooling is predicted to be significantly larger in magnitude than tropospheric warming. Researchers (ref. 1) found that by doubling the concentration of CO₂ and CH₄, the mesosphere will cool by 10 K and the lower thermosphere by 50 K, whereas the troposphere will warm by 1–3 K.

The cooling in the upper atmosphere has already begun. In the past decade, the mesosphere has cooled by 3–4 K and the mesopause by 6.5 K. This cooling exceeds the prediction of Roble and coworkers, indicating that additional cooling mechanisms are pos-

sible. It is known that the ν_2 bending mode of CO₂ can also be excited and deexcited efficiently by low-energy electron collisions. This process has been used as a source for the CO₂ laser. The large collision excitation rate constant for this process appears to compensate for the low electron number density, making this process a possible contributor to thermospheric cooling. However, at the thermospheric electron temperature of approximately 1 eV, the rate constant used in laser modeling is considered a lower estimate and has at least a factor of 2 uncertainty. More accurate modeling of thermospheric cooling requires a better data base.

The initial phase of cross-section calculations employs the Schwinger multichannel (SMC) method. Two basis sets are involved in SMC calculations: a basis to represent the target and continuum electrons and another for the calculation of Green's function matrix elements. Dunning's 9s5p1d/5s3p1d Gaussian basis is used to describe both the target and the continuum electrons, whereas the insertion calculation of Green's function matrix elements employs the original scattering basis supplemented by 10s18p9d Gaussians at the nuclear centers and 16s5p9d Gaussians at the center of mass.

In the coming year cross-section calculations over an energy range appropriate for thermosphere modeling will be performed.

References

Roble, R. G.; and Dickinson, R. E.: How Will Changes in Carbon Dioxide and Methane Modify the Mean Structure of the Mesosphere and Thermosphere? *Geophysics Research Letters*, vol. 16, no. 12, 1989, pp. 1441–1444.

Keywords

Thermospheric cooling, Electron-CO₂ collisions, CO₂ vibrational bending mode

Understanding Ion Mobility in Polymer Electrolytes for Lithium-Polymer Batteries

Investigator(s)

Richard L. Jaffe, Ames Research Center,
Moffett Field, CA 94035-1000
Grant D. Smith, University of Missouri,
Columbia, MO 65211

Other personnel involved

Harry Partridge, Ames Research Center

Objectives of the study

To develop a molecular-level understanding of the lithium ion transport process in poly(ethylene oxide) gels used as the electrolyte in lithium-polymer batteries. Such an understanding is critical to the design of optimal lithium-polymer batteries for aerospace, automobile, and electronics applications. Ab initio quantum chemistry calculations were used to determine the nature of the Li^+ -polymer interaction and molecular dynamics simulations performed on ion-polymer systems to probe the ion transport mechanism. The simulations can be carried out to determine the rate of ion transport as a function of ion concentration, cross-link density, and identity of the anion.

Progress and results

The first year of this project was spent determining an accurate force field for use in the molecular dynamics simulations of the ion-polymer systems. A previously determined force field for the polymer, poly(ethylene oxide), or PEO, was used to perform ab initio quantum chemistry calculations to determine the geometries and energetics of complexes involving Li^+ and model ether molecules such as dimethyl ether and dimethoxyethane (DME). These calculations were carried out using standard computational chemistry methods. However, one novel feature was the use of a specially derived basis set for Li^+ , which produced results that are significantly more accurate than ones obtained previously. The interaction of the cation with up to four ether molecules was studied to determine the effects of multiple solvation. The interaction of Cl^- and I^- anions with Li^+ and with the model ethers was also studied. During the current fiscal year those results will be extended to a more complex anion (PF_6^-).

The quantum chemistry results were fit to atom-ion and ion-ion pairwise functions to represent the ion-ether interactions in a form suited for use in molecular dynamics simulations. When combined with previous work for PEO, this represents the so-called force field. In order to match the quantum chemistry results, terms in the force field were included to represent polarization effects in addition to the standard coulomb, dispersion, and steric repulsion terms.

Using this force field, molecular dynamics simulations are being performed for a system of 32 $\text{H}-(\text{CH}_2-\text{O}-\text{CH}_2)_{12}-\text{H}$ polymer chains and 10 Li^+ and 10 Cl^- ions at a temperature of 450 K. The results of these simulations indicate that, on average, each Li^+ is solvated by 8 oxygen atoms from 2 different polymer chains. The presence of the Li^+ slows the self-diffusion rate of the PEO. The Li^+ and polymer have identical diffusion coefficients. On the other hand, the Cl^- anion moves much more rapidly through the polymer because it does not interact as strongly with other species.

Significance of the results

The results obtained have demonstrated that polymer electrolytes can be simulated accurately. A detailed atomistic understanding of the mechanism of cation and anion transport has been obtained. These results give confidence in the predictions of ion mobility and charge transport that will be made during the second year of the project.

Publications

Jaffe, R. L.; Smith, G. D.; and Yoon, D. Y.: Interactions of Lithium Salts with Polyethers Based upon ab initio Quantum Chemistry Calculations. Presented at the American Physical Society March Meeting, San Jose, Calif., Mar. 1995.
Smith, G. D.; Jaffe, R. L.; and Partridge, H.: A Quantum Chemistry Study of Interactions of LiCl with Model Ethers. Submitted to *J. Phys. Chem.*

Keywords

Polymer electrolytes, Ion diffusion, Lithium salts

Residential Fireplace Density Measurement Using Airborne Multispectral Scanners

Investigator(s)

Jeff Jenner, Ames Research Center,
Moffett Field, CA 94035-1000

Objectives of the study

To determine if the spatial distribution of lit residential fireplaces can be ascertained by using an airborne multispectral scanner, which permits coverage of a large area in a short amount of time (on the order of square kilometers per minute). Also, to find the most efficient way of determining lit fireplace density.

Progress and results

Evidence is mounting that particulate matter, especially smaller than 10 microns (PM10), poses a serious health risk. The San Francisco Bay Area Air Quality Management District (BAAQMD) is looking for an efficient way of determining the approximate number and spatial distribution of fireplaces and wood stoves that are in use on a given night. In the Bay Area, concentrations of PM10 are highest on cold, calm nights during December and January. Analysis of the composition of PM10 in the Bay Area as well as other urban areas suggests that as much as 40 percent is wood smoke. Currently, there are no adequate methods for estimating particulate emission from residential wood burning. Phone, mail, or door-to-door surveys have been suggested as possible methods of collecting data for developing a spatial inventory. However, surveys provide data of unknown reliability, often have low response rates, and provide only limited spatial information.

The Ames C-130 Earth Resources Aircraft may be able to use its NS001 Thematic Mapper Simulator or thermal infrared multispectral scanner (TIMS) to conduct such a survey over a large portion of the Bay Area in just a few hours. These scanners detect the amount of thermal energy *emitted* from objects on the

ground, relative to preset reference temperatures, thereby giving an indication of surface temperatures. The NS001 also detects *reflected* energy in several visible and infrared wavelength bands. With the aircraft flying at an altitude of 2500 feet above ground level (AGL), the ground resolution cell for NS001 is 1.9 square meters. Its sensor actually indicates a single average reflected or emitted energy level for that entire cell, so it cannot distinguish between different objects within the same cell. The TIMS operates on the same principle. The lowest altitude at which TIMS can operate is 4000 feet AGL, with a 3.0-square-meter ground cell resolution.

If the lit fireplaces can be easily differentiated from other thermal features on homes, either by high relative radiant temperatures or by prominence in particular wavelength bands, the data processing software could be programmed to automatically determine fireplace density for a given area. This would give the BAAQMD an inexpensive and responsive (with short notice) method of obtaining fireplace density measurements, enabling them to get correlative data for many different airborne particulate measurements.

Significance of the results

If this initial study is successful, it would introduce a new technique that could better determine the relative contributions by various sources to undesirable airborne particulate counts in urban areas. Because Ames Research Center has one of the few airborne platforms with thermal infrared scanners, this study could lead to several reimbursable projects with other state and local agencies and ultimately expand the market for commercial airborne thermal infrared imaging services.

Keywords

Remote sensing, Air quality, Fireplace

Turbulent Boundary Layer Measurements on Transport Wing Wind-Tunnel Models

Investigator(s)

Dennis A. Johnson,
Ames Research Center,
Moffett Field, CA 94035-1000
Jeffrey D. Brown,
MCAT Institute, Ames Research Center

Objectives of the study

To evaluate candidate laser Doppler velocimeter (LDV) approaches for transport wing boundary layer measurements.

Progress and results

Measurements of both the streamwise and cross-flow velocity components are needed to define the viscous boundary layers on transport wing wind-tunnel models. Moreover, these measurements must be made very close to the surface of the wind-tunnel model since the boundary layers are relatively thin. The extreme gradients in velocity within the boundary layer also place severe demands on spatial resolution. The requirements are further complicated by the need to measure separated flows.

In the current research, evaluations are made of LDV approaches that provide better spatial resolution than previous approaches, greater sensitivity to the cross-flow velocity component, and less susceptibility

to surface light scattering. Laser light scattered from the surface of the wing represents the most formidable problem. This scattered light results in additive noise, which can overwhelm the weak signals produced by the scattering of laser light from small submicron particles in the airstream. (In LDV, local instantaneous airflow velocities are deduced from the Doppler shift of laser light scattered from airborne particles.)

Laboratory studies and transonic wind-tunnel testing have established that substantial improvements in near-surface measurement performance are obtainable by modifying the surface of the wind-tunnel model and by bringing the laser beams into a tighter focus at the point of velocity measurement. Measurements within 0.1 mm of the surface have been demonstrated at transonic conditions on a wing.

Further wind-tunnel studies are planned to establish three-dimensional measurement capabilities.

Significance of the results

The capability of making accurate boundary layer measurements on wind-tunnel wing models at transonic conditions could greatly accelerate progress in the development of computational fluid dynamics tools for testing wing designs at off-design conditions.

Keywords

Boundary layers, Wings, Laser Doppler velocimetry

Validation of Engine-change Procedures through Team Task Analysis

Investigator(s)

Barbara G. Kanki,
Ames Research Center,
Moffett Field, CA 94035-1000

Other personnel involved

Diane Walter, Boeing Commercial Airplane
Company, Seattle, WA 98124

Objectives of the study

To enhance maintenance procedures through the incorporation of team task analyses. In addition, to develop assessment metrics so that team performances can be accurately and consistently evaluated. The general approach is to use the B737 CFM56-7 engine change operations as a testbed for developing the generic team task analysis system and assessment tools. Research steps include the following:

- Review accident and incident reports
- Develop collaborative plan with Boeing Commercial Airplane Company participants
- Conduct familiarization observations of engine-change activities
- Develop a model team task analysis system
- Apply the team task analysis system to the original and enhanced engine-change procedures that incorporate team process data and feedback
- Validate procedure differences through observations, interviews, and videotapes
- Refine existing performance metrics to incorporate team processes
- Write a technical report describing the team task analysis system and associated measurement system

Progress and results

Literature review of accident reports and analysis of incident reports was completed for the purpose of gathering information on team and organizational features that have been linked to incident and accidents.

Collaborative planning with Boeing participants is in process. The plan includes: 1) identifying relevant company participants; 2) obtaining existing documentation on original B737 CFM56-7 engine-change procedures; and 3) obtaining data and documentation on recent B737 engine-change updates (including timeline analyses, videotape records, and existing performance data.

Significance of the results

The literature review and incident report analyses have supported the premise that human factors problems in aircraft maintenance are highly linked to procedures and implicate more than individual maintenance personnel. "Teams" implicated in incidents come from within the maintenance organization (e.g., supervisors, inspectors, different shifts), as well as outside (e.g., flight crews, ramp personnel).

Publications

Veinott, E.; and Kanki, B. G.: Identifying Human Factors Issues in Aircraft Maintenance Operations. Poster presentation at Human Factors and Ergonomics annual meeting and poster session, San Diego, Calif., Oct. 1995.

Keywords

Team task analysis, Maintenance resource management, Crew factors in procedure design

Nonlinear Interactions between Background Disturbances and Disturbances Generated by Laminar Flow Control Devices

Investigator(s)

Lyndell S. King,
Ames Research Center,
Moffett Field, CA 94035-1000
Jonathan H. Watmuff,
MCAT Institute

Objectives of the study

To gain a fundamental understanding of the nonlinear interactions between background disturbances in laminar boundary layers, e.g., longitudinal vortices (Klebanoff modes) and disturbances introduced by laminar flow control (LFC) devices, e.g., Tollmien-Schlichting (TS) waves. To explore the conditions under which the interactions are favorable (e.g., suppression of TS wave growth) or detrimental (e.g., secondary instabilities associated with the vortices). To evaluate the usefulness of the parabolized stability equations (PSE) numerical method by performing closely coupled experimental investigations.

Progress and results

The DDF funding was awarded on June 1, 1995, and progress to date is accordingly limited. A tightly coupled numerical/experimental approach will be used. The harmonic point source (HPS) is the simplest possible form of three-dimensional (3-D) disturbance and it generates a TS wavetrain that fans out in the spanwise direction. This disturbance is representative of LFC devices (e.g., suction holes) and both measurement and computation of this case has been demonstrated. Klebanoff modes are low-frequency background disturbances that cause spanwise variations in the layer thickness and they provide an unexplained link between free-stream turbulence and transition. Klebanoff modes are analytically connected to Görtler vortices on concave walls and they

appear as cross-flow vortices in 3-D boundary layers. Techniques have been explored to introduce streamwise vortices in a controlled manner to simulate the effects of Klebanoff modes (as the background disturbance). The experimental facility consists of a dedicated, small-scale, high flow quality wind tunnel. A sophisticated high-speed computer-controlled 3-D probe positioning system has been integrated into the test section. The traverse is synchronized with a high-speed data acquisition and processing capability and all experimental procedures are totally automated under computer control. Techniques have been developed for measuring the interactions between disturbances using unprecedentedly large 3-D grids. The capabilities of a new PSE code are currently being explored. It is vital that the experiment and computation can use closely matched conditions.

Significance of the results

The drag reduction obtained by maintaining LFC over a substantial portion of a wing surface potentially offers considerable fuel savings. However, there is evidence to suggest that detrimental nonlinear interactions can occur between background disturbances and the disturbances introduced by LFC devices. These interactions remain poorly understood despite being responsible for the differences between the observed and predicted performance in practice. The proposed research will help solve the problem because a detailed understanding of the underlying physics can be used to identify the most likely cause of detrimental interactions in practical configurations.

Keywords

Tollmien-Schlichting waves, Klebanoff modes, Nonlinear interactions, Transition, Experiment, Parabolized stability equations

Ground-based Photometric Detection of Terrestrial-sized Extrasolar Planets

Investigator(s)

David Koch, Ames Research Center,
Moffett Field, CA 94035-1000
Laurance Doyle, SETI Institute,
Mountain View, CA 94043

Objectives of the study

To perform ground-based photometric observing in collaboration with the Transit of Extrasolar Planets (TEP) network to detect planets in orbit around eclipsing binary stars.

Progress and results

Observing eclipsing binaries overcomes the statistical improbability of planetary transits because the planetary orbital plane is expected to be parallel with the binary orbital plane because of precessionally induced damping (ref. 1). Observing the smallest such systems assists in overcoming the atmospheric scintillation limits on photometric detection. We are presently observing the CM Draconis system, whose equivalent stellar area is only 12 percent that of a solar-type star, allowing direct detections of transiting planets 10 times smaller in area than could be detected around solar-type stars. Significant improvement in the detectability, well below the remote manipulator system (RMS) noise, is also achieved by cross correlating the light curves with models of all possible planetary transit cases (a matched-filter signal detection algorithm). In this approach the expected quasi-periodic transit signals are “co-added” to obtain a high cumulative signal-to-noise ratio (SNR) from the individual low SNR points. With moderately good photometry (≈ 0.7 percent) using 0.9-meter ground-based telescopes, this technique should allow the detection of 87 percent of all ≥ 2 -Earth-radii planets with periods of 60 days or less at the 99.9-percent confidence level (i.e., 0.001 chance of a false alarm) within a 12-month observing period (ref. 2). In addition, giant outer planets may also be photometrically detected *without* having to await a transit. A small eclipsing binary system will be significantly displaced about a binary-planet barycenter if a giant (i.e., Jovian-mass) planet is in orbit around the system. This will cause a slow, periodic drift in the times of eclipse minima (refs. 3–4). Occasional timing of eclipse minima to within a couple seconds accuracy (using a standard Global Positioning System (GPS)) over a few years is shown to be suffi-

cient to allow a survey of eclipsing binary systems with “Jupiters” around them in about 250 such small-mass systems.

About 330 hours (about half a month; twice this from the other network telescopes) of photometric data have been obtained on the CM Draconis system that is still in the process of being reduced to light curve data via aperture photometry. The combined light curves need to be characterized for noise so that limits on detectability can be specified. With this, the matched-filter model can be run on the data to see if any cross correlations produce transiting planet candidates for prediction and observations with larger telescopes. Three such transits would constitute a confirmed detection.

Many other observatories will be admitted into the TEP network (including facilities in Arizona, China, and Russia under consideration at present). Observing will also be extended to other small eclipsing binaries (YY Geminorum, RW Doradus, and XY Leonis will be the next three targets). Observing time for RW Doradus (in the southern hemisphere) hopefully may be performed using the Antarctic 0.6-meter University of Chicago facility. Also, GPS timing will be performed on a few dozen small eclipsing binary minima for evidence of drifts in their epochs—indicative of a third mass circling the system (of Jovian mass or slightly smaller). This measurement is already being done for CM Draconis.

Near-term articles that will be published in addition to those listed above will be a “Jupiters” detection article (to be submitted to Publications of the Astronomical Society of the Pacific), the combined observing, data reduction, and light curve article from all TEP observatories for seasons 1994-1995 (to be submitted to Astronomy and Astrophysics), a paper on the new light curve of CM Draconis (to be submitted to Astronomical Journal Letters). Here, the new radii of CM Draconis A and B will be determined from the light curve, giving us the absolute brightness of CM Draconis, which also (with its already well-known mass) gives the helium content (deviations in stellar composition from pure hydrogen will affect the brightness expected for a given mass). Knowing the helium content of CM Draconis, an “unpolluted” old Population II star, may be one of the best indicators of the primordial helium abundance (giving constraints on the photon-to-baryon ratio at the time elementary particles condensed out of the Big Bang). Finally, the

first results on the evidence (or absence) of terrestrial-sized (i.e., sub-Neptune-sized) planets around CM Draconis will be submitted (likely to Science).

Eventually, when (if) transiting planets are detected, large light collecting areas will want to be employed to measure the absorption in the stellar spectrum due to the planet's atmosphere. This is presently conceivable at a reasonable investment of effort, but it would be easier than trying to measure extrasolar planetary atmospheric spectra by reflection (i.e., imaging). Thus the study of planetary characteristics could begin to be extended to other solar systems in the galaxy.

References

1. Schneider, J.; and Doyle, L. R.: Ground-Based Detection of Terrestrial Planets By Photometry: The Case for CM Draconis. *Earth, Moon, and Planets*, in press, 1995.
2. Jenkins, J. M.; Doyle, L. R.: and Cullers, D. K.: A Matched Filter Method for Ground-Based Sub-Noise Detection of Terrestrial Extrasolar Planets in Eclipsing Binaries: Application to CM Draconis. *Icarus*, in press, 1995.
3. Doyle, L. R.; Jenkins, J. M.; Deeg, H-J.; Martin, E.; Schneider, J.; Chevreton, M.; Paleologou, E.; Kylafis, N.; Lee, W-B.; Dunham, E.; Koch, D.; Blue, E.; Toubanc, D.; Ninkov, Z.; and Sterken, C: Ground-Based Observations to Detect Terrestrial and Jovian Planets Around CM Draconis. *Bull. Am. Astron. Soc.*, vol. 27, 1995, p. 1159.
4. Doyle, L. R.; Dunham, E. T.; Deeg, H-J.; Blue, J. E.; and Jenkins, J. M.: Detectability of Terrestrial Extrasolar Planets: U.C. Lick Observations of CM Draconis, *J.G.R. Planets*, in press, 1996.

Keywords

Planetary detection, Eclipsing binaries, Stellar photometry

Practical Evaluation of a New Method to Reduce Helicopter Rotor Hub Loads

Investigator(s)

Sesi Kottapalli,
Ames Research Center,
Moffett Field, CA 94035-1000

Other personnel involved

Inderjit Chopra and Judah Milgram,
University of Maryland,
College Park, MD 20742

Objectives of the study

To evaluate a new passive device (dynamically tuned blade pitch link) to reduce helicopter rotor hub loads. In addition, to evaluate an improved time-domain nonlinear elastomeric lag damper model for bearingless main rotors.

Progress and results

The research was performed using the analytical rotorcraft code UMARC (University of Maryland Advanced Rotor Code). Under this grant a modified version of UMARC was created in which it is possible to vary the pitch link damping; pitch link stiffness was also included as a parameter. The dynamically tuned blade pitch link is a device in which a rotor blade pitch link (also commonly referred to as a pushrod) is replaced by a spring/damper element. A sample study was conducted using an articulated rotor blade, the S-76 blade. Results indicated that pushrod damping in combination with reduced pushrod stiffness results in significant reductions in 4/rev fixed system hub loads. The longitudinal inplane shear was reduced by 25 percent, the roll moment by approximately 20 percent,

and the pitch moment by 25 percent. The lateral inplane and vertical shears stayed the same. At the same time, the 1/rev pushrod loads increased by about 50 percent. The design of a dynamically tuned blade pitch link may involve the redesign of a production pushrod in order to accommodate the required stiffness/damping, and any additional fatigue considerations arising from the increased 1/rev loads can be included in this redesign phase.

The second phase of this study involves evaluating an improved time-domain nonlinear elastomeric lag damper model for bearingless main rotors. This study will provide a broad understanding of the aeroelastic and aeromechanical stability characteristics, hub loads, and damper loads of bearingless main rotor helicopters.

Publications

1. Milgram, Judah; Chopra, Inderjit; and Kottapalli, Sesi: Dynamically Tuned Blade Pitch Links for Vibration Reduction. Presented at the 50th Annual Forum of the American Helicopter Society, Washington, D.C., May 1994.
2. Kottapalli, Sesi; Chopra, Inderjit; and Milgram, Judah: Dynamically Tuned Blade Pitch Links for Hub Loads Reduction. Presented at the International Exhibition and Seminar on Potential for Helicopter Development and Utilization in South Asia Pacific, Bangalore, India, Oct. 30–Nov. 1, 1995.

Keywords

Rotorcraft, Hub loads, Pushrods

Development of an Automated Telescope Balancing System for the Kuiper Airborne Observatory/Stratospheric Observatory for Infrared Astronomy

Investigator(s)

Robert W. Mah, Ames Research Center,
Moffett Field, CA 94035-1000

Other personnel involved

Alex Galvagni, Ramin Eshaghi, and
Robert Curlee, Caelum, Ames Research Center
Barry Fujii, NASA Ames Internship and Training
Program with the Foothill-DeAnza Community
College District

Objectives of the study

Kuiper Airborne Observatory (KAO) personnel have identified computer-aided telescope balancing as a needed capability that would save a significant amount of time and would improve KAO operational effectiveness. In addition, automated telescope balancing has been identified as a “critical technology need” for the Stratospheric Observatory for Infrared Astronomy (SOFIA), which will serve as the evolutionary replacement for the KAO. It is planned that SOFIA will accommodate 65 science teams per year with approximately 160 flights per year.

The problem is that a trial-and-error procedure is used to balance the KAO telescope. This procedure can be very time consuming, and requires a highly skilled, experienced technician to perform. The balancing task can take up to half a day to perform. Only a small set of technicians have acquired the necessary skills and experience to perform this difficult task. Imbalances generated in flight can be only partially compensated, sometimes not at all because the telescope balancing task is so difficult to perform efficiently and effec-

tively. A better method is needed for balancing the KAO telescope. To address these problems, an innovative noncontacting methodology that utilizes advanced adaptive neural algorithms to determine the balance parameters required to cancel telescope imbalances caused by the science instrument and its mass property changes is being developed.

Progress and results

The feasibility of using an “innovative noncontacting sensor” was demonstrated by conducting onsite sensor tests in the KAO aircraft; three-dimensional (3-D) graphics simulators of the KAO telescope were developed; dynamics equations to drive graphics simulators were developed; the feasibility of utilizing neural net methodology for telescope balancing using 3-D graphics simulators was demonstrated; the concept feasibility using a simple hardware prototype testbed was demonstrated; and construction of a high-fidelity one-half-scale prototype of the KAO telescope was initiated.

Significance of the results

Results to date indicate that the proposed concept using an “innovative noncontacting sensor” with neural net technology to balance a highly nonlinear telescope system may be feasible. Simple models and a prototype have been used. Concept feasibility will be evaluated using a high-fidelity telescope prototype that is being constructed.

Keywords

Telescope balancing, Neural net, Noncontacting sensor

Planar Doppler Velocimetry

Investigator(s)

Robert L. McKenzie,
Ames Research Center,
Moffett Field, CA 94035-1000

Objectives of the study

Flow velocities, their spatial distribution, and their temporal variations are important fundamental parameters in any aerodynamic testing program. In this project, an advanced, laser-based, optical technique called planar Doppler velocimetry (PDV) is being developed that is capable of determining three-dimensional (3-D) velocity vectors in a plane defined by a light sheet in the flow. The Doppler shift of pulsed laser light that is scattered from smoke or particles moving with the flow can be quantitatively imaged to determine an instantaneous velocity field for each laser pulse. Single-particle discrimination is not necessary, thereby making the technique applicable to facilities of any size in which adequate optical access is available, and in which aerosols can be added to the flow. In most NASA wind tunnels, the optical access provided by typical flow visualization systems will be applicable without modification, and the aerosols provided by existing vapor screen equipment or by natural vapor condensation will be suitable. In the long term, the capabilities of PDV are expected to make it a practical technique for production testing, and to foster a significant industrial interest in the technology. The fundamental objective of this work is to advance the technology of the concept to the point where it can be implemented in a large-scale production wind tunnel.

The PDV approach adopted here is a follow-on to a recently demonstrated method called Doppler global velocimetry (DGV) in which an ion-plasma, continuous-wave laser is used to obtain time-averaged velocity fields in flows that are assumed to be steady. This PDV method relies on the use of an advanced, solid state, pulsed laser to enable the measurement of instantaneous velocity fields in flows with arbitrary time dependence and turbulence. It also incorporates scientific-grade, low noise, charged coupled device (CCD) cameras to achieve highly accurate, pulsed measurements. To obtain the velocity field, the Doppler frequency shift of light scattered by aerosols moving with the flow is detected everywhere in the field of view by imaging through a sharp-edged spectral filter that is created by molecular iodine vapor in

an optical cell. Frequency-shifted light is transmitted by the filter differently from unshifted light. In its full implementation, CCD cameras view the light sheet through molecular filters from three directions. After processing, the gray levels in each set of corresponding pixels are a measure of three separate velocity field components from each observed field point in the light sheet.

Progress and results

A comprehensive feasibility study, including validating experiments, has been performed and reported that provides a detailed analysis of the single-pulse measurement uncertainties for PDV using a CCD imaging system. The following issues are reported:

An optical configuration is described and demonstrated that replaces the two-camera system originally used for the measurement of each velocity component with an optical arrangement that permits the use of a single camera. This approach makes more reasonable the use of high-cost, scientific grade, CCD cameras that are shown to be necessary to obtain accurate measurements from a single laser pulse.

A PDV signal analysis is formulated that highlights the role of the filter response function. The accurate frequency calibration and stability of the response function is shown to be a critical requirement for accurate velocity measurements. The analysis also demonstrates the need to monitor the pulsed laser frequency in conjunction with the frequency of the Doppler-shifted scattered light. Particle-to-surface scattering and multiple-particle scattering are discussed as potential sources of systematic errors.

An accurate model of the iodine vapor spectrum is developed and used in combination with experimental spectra to calibrate the frequency scale of the iodine filter response function. The spectral model is also used to identify the most appropriate spectral feature for use as a filter and to determine the optimum filter design and operating conditions.

PDV measurements of the surface velocity of a rotating wheel are described that validate the signal analysis concepts and show that velocity measurements can be obtained with uncertainties that are limited by the ± 1 count uncertainty of a 12-bit analog-to-digital (A/D) conversion. Point measurements were made of the wheel surface speed from 5 to 56 m/s with a consistent root mean square (rms) error of ± 2.5 m/s for all speeds above 10 m/s.

The intrinsic noise sources in a radiometric measurement using a CCD detector array are characterized and a description is given of their influence on the measurement uncertainty of Doppler shift for a given signal level. The requirement for a scientific-grade, cooled, slow scan, CCD system with at least 12-bit A/D conversion becomes apparent. The results show that by using a 16-bit CCD system, velocity measurements should be possible with a dynamic range of over 300 MHz (≈ 200 m/s) and a resolution of 2 MHz (≈ 1.5 m/s).

To determine the signal levels that can be expected in an aerodynamic test situation, the scattering properties are characterized for aerosols that are practical for aerodynamic flow seeding. The results show that opaque particles are the least sensitive to variations in particle size distributions or observation direction and that their essential scattering properties for this application can be described solely by the optical extinction depth of the aerosol. Using this easily measured characteristic, the PDV measurement uncertainty is predictable for most experimental situations.

The use of opaque scattering particles has been shown to minimize the sensitivity of the scattering signal to particle distributions and observation direction. That behavior, together with concerns regarding the possible anomalous effects of multiple-particle scattering among non-absorbing, highly refracting, particles, encourages the use of opaque smoke particles as the PDV seed material.

Finally, the maximum observation distances, or test facility sizes, for which selected signal levels and their related measurement uncertainties can be achieved are estimated for a range of practical test situations. The estimates assume parameters that are readily obtainable from commercially available laser and CCD camera equipment. The results predict that single-pulse, PDV measurements with uncertainties as low as 2 m/s should be possible in aerodynamic test facilities for ranges up to at least 20 meters. This performance pertains to laser light sheets with a height that is kept proportional to the facility size by equating it to 1/10 the distance to the sample volume. The facility size or observation range can be extended to more

than 100 meters by accepting velocity uncertainties to 8 m/s or by reducing the height of the laser light sheet.

Since publication of the above study, a developmental laboratory instrument has been assembled that contains a single CCD camera and allows the measurement of one component of velocity in a bench-top air jet. In addition, the core elements of the image processing software have been completed. In the next year, they will be assembled into a complete data analysis package that will autonomously convert scattering particle images into velocity fields. The one-component system will then be used to verify the PDV measurement capabilities by comparing its data with the jet flow properties measured by conventional means. Finally, in the next year, the system will be extended to two velocity components by the addition of a second camera. Completion of this work will lead to the fabrication of a three-component system and its demonstration in a full-scale wind tunnel currently in use for aerodynamic research in the Fluid Mechanics Laboratory.

Significance of the results

So far, the results of this work have shown that single-pulse PDV measurements can be expected to provide accurate 3-D velocity vector measurements in both small and large test facilities, with temporal and spatial resolution that is sufficient for most aerodynamic testing objectives. Its advantages over existing velocity measurement techniques appear to be significant for applications to large aerodynamic facilities.

Publications

McKenzie, R. L.: Measurement Capabilities of Planar Doppler Velocimetry Using Pulsed Lasers. AIAA Paper 95-0297, presented at the AIAA 33rd Aerospace Sciences Meeting and Exhibit, Reno, Nev., Jan. 9-12, 1995. (Accepted for publication in *Applied Optics*, 1996.)

Keywords

Aerodynamic measurements, Three-dimensional velocimetry, Doppler velocimetry

A Microwave-Pumped GaAs Far Infrared Photoconductor

Investigator(s)

Robert E. McMurray, Jr.,
Ames Research Center,
Moffett Field, CA 94035-1000
Jam Farhoomand,
Orion TechnoScience,
Palo Alto, CA 94036

Other personnel involved

Nick Scott, Trans-Bay Electronics, Inc.,
Ames Research Center

Objectives of the study

To develop a method for increasing the strength of the long-wavelength response of existing far infrared (IR) detectors without an increase in leakage, current, or noise. This is to be accomplished by operating the detectors very cold for low leakage, and replacing the thermal pumping normally needed for long-wavelength response with microwave pumping. The ultimate goal of the project is to provide a mechanism for detector operation for NASA- and European Space Agency (ESA)-planned satellites requiring low-noise long-wavelength IR detectors.

Progress and results

An extensive study had been previously performed by the investigators to ascertain the suitability of GaAs photoconductor for the far IR spectral region. The study included the determination of the spectral response of several GaAs samples at a series of temperatures, generally in the range of 4.2 to 1.7 K (see fig. 1). The high leakage current and noise at the higher temperatures demonstrate the need for operating cold. The exponential fit of the decay of the long-wavelength response with decreasing temperature shows that it is essential to provide microwave pumping at cold temperatures.

All microwave components have been procured (horns, waveguides, detector mount and antenna, and 110-GHz Gunn oscillator). Machining has been performed on parts required to modify a standard cryogenic dewar to accommodate the feed and reception horns, 110-GHz waveguides, and detector antenna and mounting block for microwave pumping operation at temperatures of <2.5 K. The ongoing investigation

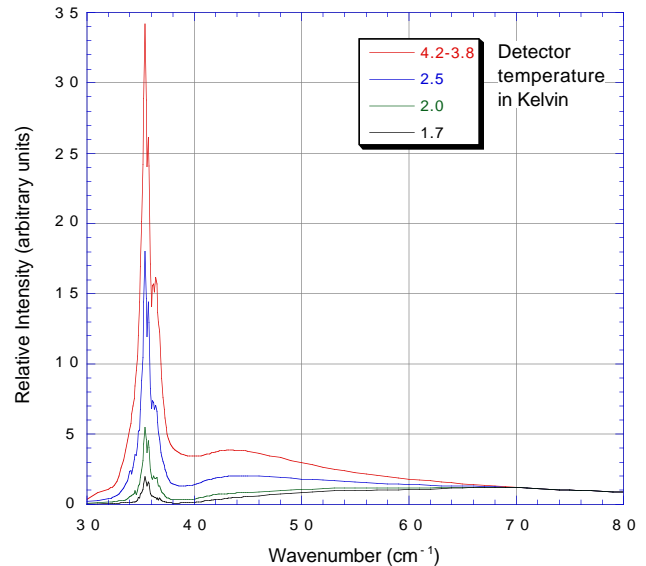


Figure 1. GaAs spectral response vs. temperature normalized to the continuum response at 80 cm^{-1} .

requires fitting of microwave equipment with GaAs detector sample to the dewar, followed by a series of microwave pumping experiments. This series will ultimately determine the optimal frequency and power of applied microwaves for lowest noise and best signal in the far IR.

Additional Gunn oscillators operating at lower microwave frequencies of 21 to 23 GHz have been obtained for testing of direct pumping of GaAs photoconductor using internal photon multiplication due to noncentrosymmetry in the crystal structure.

Significance of the results

The results will be used for optimization of detectors proposed for long-wavelength satellite missions. Such missions are already proposed by both NASA and ESA using long-wavelength photoconductors. These would be greatly improved by using the results of this development, and would result in enhanced scientific data.

Keywords

GaAs photoconductors, Far infrared detectors, Photoconductors

Design Optimization Using Automated Differentiation and Parallel Decomposition

Investigator(s)

Hirokazu Miura,
Ames Research Center,
Moffett Field, CA 94035-1000
Ilan Kroo,
Stanford University,
Palo Alto, CA 94305-4035

Other personnel involved

Steve Altus,
Stanford University,
Palo Alto, CA 94305-4035

Objectives of the study

Highly complex and computationally intensive, aerospace design problems involve hundreds of analyses and thousands of variables. In order to apply multi-disciplinary design optimization to such problems, efficient means to structure and manage the entire problems are necessary. A promising strategy is decomposition of the problems into several independent subproblems, which communicate only with the optimizer. This process introduces many new variables and constraints, increasing the number of gradients needed for optimization. For this strategy to be practical, ways to more efficiently solve decomposed optimization problems must be found. This study explores two possibilities toward this end: automatic differentiation and parallel optimization.

Progress and results

A sample aircraft optimization problem was used to test both automatic differentiation and decomposed parallel optimization.

ADIFOR, an automatic differentiation package for FORTRAN codes, was applied to the sample problem. A convergence history is shown in figure 1, in which the use of ADIFOR gradients is compared with the use of standard finite-difference gradients. ADIFOR provides increased computational efficiency, but it does not resolve all of the issues associated with decomposition.

A decomposed version of the sample problem, shown in figure 2, has been successfully optimized in parallel, with each subproblem on a different node of a heterogeneous, distributed network. Information transfer between the different computers was done

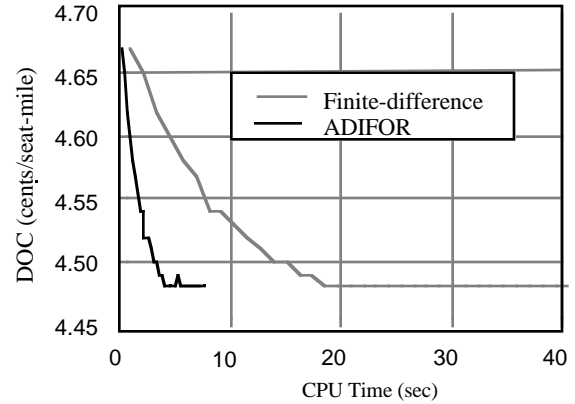


Figure 1. Convergence history for ADIFOR vs. finite-difference gradient calculation on aircraft optimization. (CPU: central processing unit.)

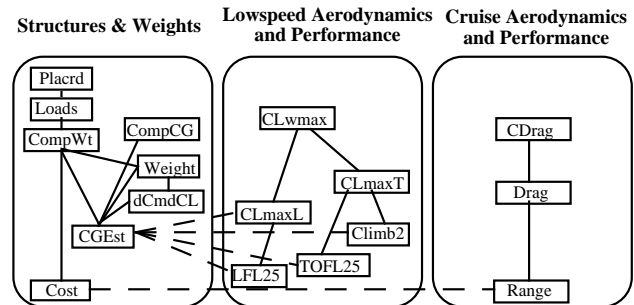


Figure 2. Aircraft synthesis problem decomposed into three subproblems by a genetic algorithm-based tool.

twith file-sharing. In order to increase efficiency, work is in progress to convert to using parallel virtual machine (PVM) for communications.

Significance of the results

Methods for increasing the efficiency of decomposed numerical design optimization problems were demonstrated. These increases make it feasible to use the complex analyses necessary for accuracy in aerospace design problems, and to decompose the problem into independent subproblems to ease the development and maintenance of large multidisciplinary analyses.

Publications resulting from study

Altus, S.; Kroo, I.; and Gage, P: A Genetic Algorithm for Scheduling and Decomposition of Multidisciplinary Design Problems. ASME-DAC-95-141, presented at 21st ASME Design Automation Conference, Boston, Mass., Sept. 17-20, 1995.

Keywords

Aircraft design, Collaborated design, Automatic differentiation

A Search Technique for Discovering Earth-crossing Comets from Meteor Stream Outbursts and Determining Their Orbits in Space

Investigator(s)

David Morrison and Peter Jenniskens,
Ames Research Center,
Moffett Field, CA 94035-1000

Other personnel involved

H. Betlem, H. Mostert, M. C. de Lignie, and
K. Jobse, Dutch Meteor Society
I. Yrjola, Kuusankoski, Finland

Objectives of the study

Impacts of near-Earth comets on Earth are a potential danger. Some 40 percent of objects that could hit the Earth are comets. Proposed near-Earth asteroid searches will detect only those long- and intermediate-period comets that happen to be in the inner solar system during the search. The objective of this study is to find long- and intermediate-period comets that pass the Earth within less than 0.01 AU by observing their meteoroid signature. Comets shed dust particles (meteoroids) while in the inner solar system. These particles spread along the comet orbit because small ejection velocities cause large changes in orbital period. On the other hand, these particles do not move far away from the comet orbit at the Earth's position. Hence, occasionally a short-duration meteor outburst occurs when the Earth crosses the dust stream. The outburst betrays the presence of the comet and allows determination of the comet orbit. These meteor outbursts occur typically once every 10–16 years for a given stream. Meteor rates can go up to 100–1000 per hour for a brief period of time (tens of minutes to tens of hours). This study explores possibilities to detect such meteor outbursts, measure orbital elements of individual meteoroids, and compare the results with historic apparitions of comets.

Progress and results

The normal annual activity of 49 meteor streams was determined. By using this as a reference frame, an inventory was made of past accounts of enhanced meteor activity that could be a meteor outburst. Four outburst streams were identified as “far-comet type,” that is, they show outbursts when the comet is far from perihelion (as opposed to “near-comet type,” when meteor outbursts coincide with the return of the

comet to perihelion). Thirteen other streams are most likely of the far-comet type, but none of these has a known associated parent object. The goal of this study is to find orbital elements of these streams.

Radio forward meteor scatter has been found useful for detecting enhanced levels of meteor activity in order to find other such outbursts. Using existing techniques and the voluntary effort of amateur meteor observers, a beginning has been made to employ such systems at widely separated sites on Earth. In order to cover all possible meteor streams at all hours of the day, at least six stations are needed in a Global Meteor Scatter Network. Current stations are in Finland and California. Meteor outbursts were recorded during the Leonids 1994, Ursids 1994, and Perseids 1995.

A mobile and versatile two-station 35-mm camera network was built; it is equipped with f1.8 50-mm optics, a crystal-driven rotating shutter, and heating ribbons, all operated from a car battery. The network has been used on seven occasions when there was an opportunity to capture a meteor outburst. The first orbital elements of outburst meteors were obtained during the 1994 Perseids on Aug. 12. The orbital elements do resemble the (known) parent comet P/Swift-Tuttle. No further efforts proved successful.

A similar network of image-intensified cameras is being built. This system is expected to allow the measurement of orbital elements of streams rich in faint meteors. A meteor processing station has been set up for astrometry and orbital element calculations.

Amateur astronomers have participated at various stages in this project. The radio meteor scatter stations are owned and run by amateur observers, and multistation photographic networks were operated with the support of 5–10 amateur astronomers of local astronomical organizations. In addition, meteor observing techniques have been applied that were developed by members of amateur meteor organizations.

Significance of the results

Progress has been made in identifying far-comet-type outbursts and understanding the cause of these events. Recurrence of far-comet-type outbursts was found to be related to planet positions. A stream has been developed where gravitational perturbations

occasionally direct a narrow trail of dust in the direction of the Earth.

It has been demonstrated that a multistation camera network can successfully be tested on near-comet-type outbursts because these outbursts occur in a series and can, therefore, be anticipated. However, anticipation of far-comet-type outbursts remains difficult because of the intrinsic narrow width of these streams. Measurement of orbital elements of far-comet-type outburst meteors requires persistence. Important experience has been obtained that will help in the further development of suitable imaging systems that are optimized for the detection of outburst meteors.

Publications resulting from study

1. Jenniskens, P.: Meteor Stream Activity. I. The Annual Streams. *Astron. and Astrophys.*, vol. 287, 1994, pp. 990–1013.
2. Jenniskens, P.: High Leonid Activity on November 17–18 and 18–19, 1994. *WGN, the J. IMO*, vol. 22, 1994, pp. 194–198.
3. Jenniskens, P.: Meteor Stream Activity. II. Meteor Outbursts. *Astron. and Astrophys.*, vol. 295, 1995, pp. 206–235.
4. Jenniskens, P.: Good Prospects for a Monocerotid Outburst in 1995. *WGN, the J. IMO*, vol. 23, 1995, pp. 84–86.
5. Jenniskens, P.: Meteor Stream Activity. III. Measurement of the First in a New Series of Leonid Outbursts. *Meteoritics*, Mar. 1996.
6. Jenniskens, P.: The First in a New Series of Leonid Outbursts. In *Physics, Chemistry and Dynamics of Interplanetary Dust*. IAU Coll., vol. 150, B. A. Gustafson, et al., eds. (submitted), 1995.
7. Jenniskens, P.: Meteor Stream Activity. IV. An Observational Link between Planetary Perturbations and the Periodic Nature of the Aurigids, Lyrids, and Other Far-comet Type Meteor Outbursts. *Astron. and Astrophys.* (submitted), 1996.

Keywords

Meteors, Meteor imaging, Meteor scatter

Ultra-light Entry Vehicle Development

Investigator(s)

Marcus S. Murbach and Demetrius Kourtides,
Ames Research Center,
Moffett Field, CA 94035-1000

Objectives of the study

To develop the technologies related to a low-ballistic-coefficient entry and delivery system.

Progress and results

Considerable progress was made on the development of the ultra-light entry system concept. The general areas of work included a) theoretical development , b) prototype hardware development, and c) mission concept development.

In terms of theoretical development, several computational tools were used to refine the concept. First, the dynamics of atmospheric entry were explored by varying entry velocity, flightpath angle, and ballistic coefficient. The heating calculation was tuned to approximate the heating at the stagnation point. A computational fluid dynamics (CFD) tool was then used to calculate the flow field and the corresponding pressure /heating distributions along the streamline. These results were compared to the

listed upper use temperatures for the various candidate materials that are being examined. The first-order design margins were then derived from the various calculations. These margins indicated that, for the baseline Mars mission case, there exist comfortable design margins either in growth of the ballistic coefficient or in terms of the reduction in diameter of the entry vehicle forebody.

A full-scale prototype of one of the probe concepts and the accompanying (and critical) ejection mechanism concept were constructed, enabling an investigation of the manufacturing and design processes. The ejection mechanism in particular was found to work as planned, and it fit within the desired volume constraints. Preparation was also begun for the next phase of instrumenting a scaled version of the current mechanical design in anticipation of drop tests.

The mission concept is also maturing. Discussions were begun with a potential partner such that the effort can be included in one of the future Discovery proposals. The effort has focused on various mission elements and system interfaces with the probe bus.

Keywords

Atmospheric entry, Planetary missions

Using Ecosystem Science and Technology to Balance the Conservation of Water Supply and Native Hawaiian Rainforests

Investigator(s)

Robyn Lee Myers, Ames Research Center,
Moffett Field, CA 94035-1000

Objectives of the study

Maui's native rainforests are among the most imperiled in the world, containing one-third of Hawaii's rare and endangered species. Research has shown that native species are highly susceptible to displacement by the invasion of nonnative species. Alien species have been shown to affect ecosystem function, community structure, and population dynamics. The mission of the East Maui Watershed Partnership (EMWP) is to protect the East Maui watershed from degradation by pooling expertise and other resources to plan, fund, and implement an active watershed-management program.

With the cooperation of the State of Hawaii and the Nature Conservancy of Hawaii, a multiscale study of the spread of alien plant species into the native rainforests of windward East Maui is being conducted. The East Maui watershed is managed by seven land owners, who formed the EMWP. The research focuses on two priorities from the EMWP management plan, which was based on recommendations made by the U.S. Forest Service: 1) Determine the specific steps needed to develop an adequate inventory of vegetation and species in the watershed in order to provide a starting point for ongoing and long-term monitoring; 2) Provide a strategy to prevent new weeds from entering the watershed area and target those species that pose the greatest threat to native species. The EMWP understands that at the heart of the watershed are the native rainforest ecosystems, which support a host of native and endemic species and form the basis of the present and future water supply for the island of Maui.

Using a landscape and systems ecology approach, the research was designed as a multiscale study to address the EMWP priorities, providing an integrative approach for identifying, detecting, and predicting changes related to alien species spread into Hawaii's native forests. Multiscale refers to areal extent, resolution of data collection tools, and species detail, for three scales: The macroscale is a coarse-grained landscape analysis of the entire watershed (40,479 Ha),

using thematic mapper images and aerial photos to classify general community types; the mesoscale is a medium-grained landscape analysis of a focus area (Waikamoi focus area – 30 Ha), examining current and historic aerial photographs over time to map change in canopy species; and the microscale is a fine-grained field verification of canopy and understory species in permanent Hawaiian bird survey plots and transects. The research will focus on the following questions, increasing current knowledge of landscape ecology's ability to address conservation management issues: 1) Is the presence and extent of alien species related to land use (including natural or human disturbances and preservation)? 2) Can canopy cover interpreted from historic aerial photos be used to identify species change (alien species spread) in native forest? and 3) At what spatial scale is the change in canopy species composition most obvious?

Previous research has suggested that the presence and extent of alien species are related to disturbance, whether the result of human land use or natural events. The first goal is to identify areas where aliens are posing the most immediate threat of spread into native areas, and the possible relationship to management policy and other landscape variables. A gap analysis of the macroscale data will be analyzed in the geographic information system (GIS) software ARC/INFO, comparing agency landuse policies with the presence of native and alien vegetation cover to identify gaps in protection of native forest. The second goal is to show how the vegetation canopy structure has changed over time, in particular, the change in the percent of alien and native species. The third goal is to identify what landscape features and species assemblage information can be detected at each scale. The abilities and limitations of the three scales of observation to detect landscape features and vegetation patterns will be compared and analyzed.

Progress and results

Funding to date has been provided by the National Biological Survey (NBS), the Nature Conservancy of Hawaii, the Charles A. and Anne Morrow Lindbergh Foundation, and the NASA Ames Research Center. Time, expertise, use of computer equipment, and digital space have been donated to the Nature Conservancy by Advanced Mapping Technologies of

Belmont, California, for the aerial photo time series portion of this work. The present work involves direct collaboration with the State of Hawaii, Department of Land and Natural Resources, the Nature Conservancy of Hawaii, and Federal agencies represented in Hawaii.

This research emphasizes the use of Environmental Systems Research Institute, Inc. (ESRI), ARC/INFO, and ArcView GIS software, and use of the internet and the World Wide Web for the exchange of data and information to facilitate long-distance collaboration.

Work on objective 1 (the gap analysis) has been completed and is under review for publication.

Publications

Myers, Robyn Lee: Bridging the Isolation Gap: Hawaiian Interagency GIS Collaborations Using the Internet. Accepted for publication, 1996 Geo Info Systems.

Myers, Robyn Lee: Part I - Gap Analysis of the Windward East Maui Watershed. Submitted to University of California, Davis, Dissertation Committee. Planning to submit to scientific journal based on their recommendation, 1996.

Myers, Robyn Lee: Balancing Ecosystem Science with a Multi-Scale Approach: The Tri-Scale Convergent Hierarchy. Invited paper, abstract submitted to The 20th Anniversary Publication of the Lindbergh Foundation, 1997.

Myers, Robyn Lee: Historical Review of the East Maui Watershed. Biological Summary and Land Use History for the East Maui Watershed Area, The Nature Conservancy of Hawaii, East Maui Watershed Partnership, Jan. 1996.

Myers, Robyn Lee: A Conceptual Framework for Studies in Landscape Ecology: The Tri-scale Convergence Hierarchy. In Issues in Landscape Ecology, Susan Ustin, ed., Springer-Verlag, 1996.

Keywords

Watershed, Geographic information system, Landscape ecology, Remote sensing, Ecosystem, Management, Hawaii

A New Method for Measuring Cloud Liquid Water Using Near Infrared Remote Sensing

Investigator(s)

Peter Pilewskie,
Ames Research Center,
Moffett Field, CA 94035-1000

Objectives of the study

To develop cloud remote sensing methods for inferring the liquid water content (LWC) of clouds, which includes the subsequent development of experimental and theoretical tools necessary for cloud property retrievals. Because the LWC in clouds is so crucial in the regulation of the Earth's hydrological cycle and therefore has direct climate implications, this effort to use a near infrared (NIR) remote sensing technique was initiated. NIR measurements of clouds had been used in past studies to infer cloud properties such as particle size, cloud thickness, and thermodynamic phase, with varying degrees of success. The objectives of this study are to use a similar approach in determining cloud water content by measuring the NIR solar spectrum transmitted through clouds and deriving the relationship between that spectral information and cloud water content.

Progress and results

A spectroradiometer system consisting of three independent monochromator-detector units was developed to achieve spectral coverage from 0.4–2.5 μm , 10-nm resolution, and 1-mrad field of view. These instruments were deployed at a surface site during a multi-agency field experiment. The data collected included measurements from aircraft in situ sensors and remote sensors, crucial for testing the new retrieval method in the DDF-funded study. Aircraft measurements of cloud particle size and water content and surface-based microwave measurements of integrated LWC are two significant data sets that will aid in the comparison of results. Over 200 hours of transmission data were obtained during the experiment, under a variety of meteorological and cloud-type conditions.

The field experiment provided a large and comprehensive data set for the development of the LWC remote retrieval algorithm. Aside from the LWC retrieval work, however, these measurements were used to infer cloud water phase (liquid or ice, the most crucial information for determining a cloud's likeli-

hood to precipitate), cloud optical thickness, and particle size. Multiwavelength analysis is necessary to separate the information content on particle size, cloud thickness, τ , and water phase, and it is similar to current aircraft and satellite cloud retrieval algorithms. Particle size and optical depth are sufficient to determine the integrated cloud water path, but the innovative effort of this research is to obtain a radiatively effective LWC (units mass/volume), a much more climatically useful parameter.

Asymptotic formulae provide an effective means of closely approximating the qualitative and quantitative behavior of transmission (and reflection) computed by more laborious detailed methods. Relationships derived from asymptotic formulae were applied to measured transmission spectra to test objectively the internal consistency of data sets acquired during the field program and they confirmed, rather dramatically, the quality of the measurements. However, these relationships appear to be very useful in themselves, not merely as a quality control measure, but also as a potentially valuable remote-sensing technique in its own right. One further benefit from this analysis has been the separation of condensed water (cloud) and water vapor transmission. The capability of deriving this additional water vapor path within cloud as a function of cloud height and geometric depth will determine the ability to derive LWC. By retrieving cloud optical thickness, τ , and particle size, r , the integrated cloud water path can be derived; the additional height information will facilitate the retrieval of LWC. The Arizona program data set will provide ground-truth verification.

Publications resulting from study

Reining, R.; Uttal, T.; Kropfli, R.; Eloranta, E. W.; Piironen, P.; Piironen, A.; Brientjes, R.; and Pilewskie, P.: Hydrometeor Distinction with Radar, Lidar, Passive Spectro-Radiometer and Aircraft Measurements in a Winter Storm. Paper presented at the International Union of Geodesy and Geophysics, XXI General Assembly, Boulder, Colo., July 2–14, 1995.

Keywords

Remote sensing, Clouds and climate

Computation of the Low-temperature Rate Constants for the Reaction $\text{HO}_2 + \text{O}_3 \rightarrow \text{OH} + \text{O}_2 + \text{O}_2$

Investigator(s)

David W. Schwenke,
Ames Research Center,
Moffett Field, CA 94035-1000
Stephen P. Walch,
Thermosciences Institute,
Ames Research Center

Objectives of the study

To compute the rate of the title reaction as a function of temperature. The temperature range of interest is 200–300 K, where the Arrhenius plot shows curvature. This will allow reliable extension of the experimental measurements down to the temperature range required for modeling studies of the Earth's atmosphere. The computation of the rate coefficient requires the characterization of the potential energy surface (PES) for the reaction, the analytic representation of the PES in the regions important for the nuclear dynamics, and finally the simulation of the nuclear dynamics as a function of temperature.

Progress and results

The first phase of this study, the determination of the PES using ab initio electronic structure techniques, is well under way. A schematic representation of the PES is shown in figure 1. The HO_2 and O_3 pass over a barrier of about 13 kcal/mol to form an initial HO_5 complex. The HO_5 complex is only slightly bound with respect to reactants and has only a very small barrier to decomposition to $\text{HO}_3 + \text{O}_2$. In turn, HO_3 has only a small barrier to dissociation to $\text{HO} + \text{O}_2$. Thus, the net reaction is $\text{HO}_2 + \text{O}_3 \rightarrow \text{HO} + \text{O}_2 + \text{O}_2$.

The stationary points corresponding to $\text{HO}_2 + \text{O}_3$, HO_5 , $\text{HO}_3 + \text{O}_2$, $\text{OH} + \text{O}_4$, and $\text{OH} + \text{O}_2 + \text{O}_2$ have been determined, and the potential energy along the reaction path connecting the stationary points has been computed. Additional work needs to be carried out to explore another pathway to the HO_5 complex, which involves a cyclic saddle point geometry.

Significance of the results

In the initial consideration of the title reaction, the curvature of the Arrhenius plot was attributed to the

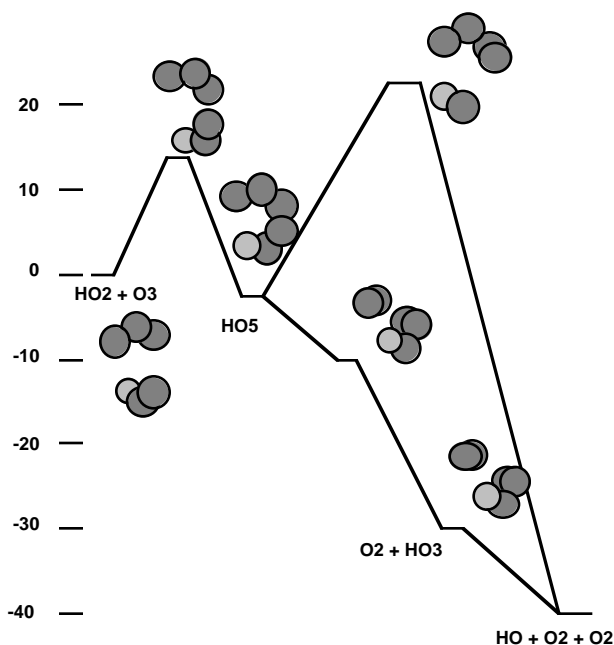


Figure 1. Schematic potential energy surface for $\text{HO}_2 + \text{O}_3$. Energies are in kcal/mol with respect to $\text{HO}_2 + \text{O}_3$.

competition of a direct reaction path, which gives rise to a negative slope, and an association pathway with a long-lived intermediate, which gives rise to a positive slope. The current calculations have characterized the association pathway. The direct pathway probably corresponds to the second pathway to the HO_5 complex mentioned above (which still needs to be characterized). It is probable that the curvature in the Arrhenius plot is due to a competition between these two pathways with different negative slopes. This is different from the original conjecture in that both pathways involve a short-lived HO_5 complex. To prove this conjecture, it will be necessary to locate the second reaction path and carry out the nuclear dynamics calculations.

Keywords

Ozone depletion, Potential energy surfaces, Reaction rates

A New Method to Test Rotor Hover Performance

Investigator(s)

Mark Silva and Frank Caradonna,
Aeroflightdynamics Directorate,
U.S. Army Aviation and Troop Command,
Ames Research Center,
Moffett Field, CA 94035-1000

Objectives of the study

To evaluate a new rotor hover test technique based on treating hover as a limiting case of the more general condition of vertical climb. A climb condition will be simulated by testing a rotor on a horizontal axis (axial flight) test rig in the settling chamber of the 7- by 10-Foot Subsonic Wind Tunnel. The low-speed tunnel flow should stabilize the wake and suppress flow recirculation and thus allow the acquisition of high-quality climb performance data. The data could then be extrapolated to provide hover performance data of unusual quality.

Progress and results

Design and layout of the truss structure that will support the rotor drive, controls, and balance measurement system in an axial flight mode in the 7- by 10-Foot Subsonic Wind Tunnel settling chamber have been completed. The rig, designated as the rotor axial flight test rig (RAFTR), is being fabricated inhouse. Site preparation has begun with installation targeted for early 1996.

Significance of the results

During the next fiscal year axial flight testing of a four-bladed model-scale rotor will be performed on the RAFTR test rig. Hover performance derived by extrapolation of the climb performance will be compared to hover data measured previously by conventional methods to determine the merits of the proposed technique.

Keywords

Hover performance, Vertical climb, Rotor test

REPORT DOCUMENTATION PAGE			Form Approved GSA No. 0704-0188	
Public reporting burden for this collection of information is estimated to average 1 hour per response, including the time for reviewing instructions, searching existing data sources, gathering and maintaining the data needed, and completing and reviewing the collection of information. Send comments regarding this burden estimate or any other aspect of this collection of information, including suggestions for reducing the burden, to Washington Headquarters Service, Directorate for Information Operations and Reports, 1215 Jefferson Davis Highway, Suite 1204, Arlington, VA 22202-4302, and to the Office of Management and Budget, Paperwork Reduction Project (0704-0188), Washington, DC 20503.				
1. AGENCY USE ONLY (Leave blank)	2. REPORT DATE March 1996	3. REPORT TYPE AND DATES COVERED Technical Memorandum		
4. TITLE AND SUBTITLE Director's Discretionary Fund Report for Fiscal Year 1995			5. FUNDING NUMBERS 274-50-61	
6. AUTHOR(S) Ames-Moffett Investigators				
7. PERFORMING ORGANIZATION NAME(S) AND ADDRESS(ES) Ames Research Center Moffett Field, CA 94035-1000			8. PERFORMING ORGANIZATION REPORT NUMBER A-960214	
9. SPONSORING/MONITORING AGENCY NAME(S) AND ADDRESS(ES) National Aeronautics and Space Administration Washington, DC 20546-0001			10. SPONSORING/MONITORING AGENCY REPORT NUMBER NASA TM-110376	
11. SUPPLEMENTARY NOTES Point of Contact: John T. Howe, Ames Research Center, MS 200-16, Moffett Field, CA 94035-1000; (415) 604-5500				
12a. DISTRIBUTION/AVAILABILITY STATEMENT Unclassified-Unlimited Subject Category - 99			12b. DISTRIBUTION CODE	
13. ABSTRACT (Maximum 200 words) This technical memorandum contains brief technical papers describing research and technology development programs sponsored by the Ames Research Center Director's Discretionary Fund during fiscal year 1995 (October 1994 through September 1995). An appendix provides administrative information for each of the sponsored research programs.				
14. SUBJECT TERMS Director's Discretionary Fund, Space science, Life science, Aeronautics, Space and terrestrial applications			15. NUMBER OF PAGES 80	
			16. PRICE CODE A05	
17. SECURITY CLASSIFICATION OF REPORT Unclassified	18. SECURITY CLASSIFICATION OF THIS PAGE Unclassified	19. SECURITY CLASSIFICATION OF ABSTRACT	20. LIMITATION OF ABSTRACT	